Kaikoura Earthquake Short-Term Project

Title: Landslide inventory and landslide dam assessments

Leaders: C. Massey and S. Dellow

Organisation: GNS Science

Total funding (GST ex): $250,000

Kaikoura Earthquake Short-Term Project: Landslide inventory and landslide dam assessments

CI Massey, D Townsend, S Dellow, B Lukovic,
B Rosser, G Archibald, M Villeneuve, J Davidson,
K Jones, R Morgenstern, D Strong, B Lyndsell,
J Tunnicliffe, J Carey, S McColl

GNS Science Report 2018/19
June 2018

GNS SCIENCE
TE PŪ AO

DISCLAIMER

The Institute of Geological and Nuclear Sciences Limited (GNS Science) and its funders give no warranties of any kind concerning the accuracy, completeness, timeliness or fitness for purpose of the contents of this report. GNS Science accepts no responsibility for any actions taken based on, or reliance placed on the contents of this report and GNS Science and its funders exclude to the full extent permitted by law liability for any loss, damage or expense, direct or indirect, and however caused, whether through negligence or otherwise, resulting from any person's or organisation's use of, or reliance on, the contents of this report.

BIBLIOGRAPHIC REFERENCE

Massey CI, Townsend DB, Dellow GD, Lukovic B, Rosser BJ, Archibald, GC, Villeneuve M, Davidson J, Jones KE, Morgenstern R, et al. 2018. Kaikoura Earthquake Short-Term Project: landslide inventory and landslide dam assessments. Lower Hutt (NZ): GNS Science. 45 p. (GNS Science report; 2018/19). doi:10.21420/G2FP82.

Massey, Townsend, Dellow, Lukovic, Archibald, Rosser, Jones, Morgenstern, Strong, Lyndsell and Carey, GNS Science, PO Box 30369, Lower Hutt, New Zealand

Villeneuve and Davidson, Department of Geological Sciences, University of Canterbury, Private Bag 4800, Christchurch 8140, New Zealand.

McColl, Physical Geography Group, School of Agriculture and Environment, Massey University. Private Bag 11222, Palmerston North 4412, New Zealand.

Tunnicliffe, Auckland University, Science Centre 302 - Bldg 302, Level 7, Room 749, 23 Symonds St, Auckland, 1010, New Zealand.

www.gns.cri.nz

ISSN 2350-3424 (online)
ISBN 978-1-98-853082-6 (online)
http://dx.doi.org/10.21420/G2FP82

CONTENTS

ABSTRACT ..... **IV**

KEYWORDS ..... **IV**

1.0 INTRODUCTION **1**

2.0 KEY FINDINGS **3**

2.1 Landslide inventory mapping 3

2.1.1 Examples of landslides triggered by the earthquake 5

2.1.2 Preliminary analysis of landslide inventory results 11

2.2 Landslide dams 14

2.2.1 Regional-scale landslide dam assessments 18

2.2.2 Site-specific landslide assessments 18

3.0 DISCUSSION **23**

3.1 Who has used the data 23

3.2 Future work 28

4.0 ACKNOWLEDGMENTS **29**

5.0 REFERENCES **29**

FIGURES

Figure 2.1 Inset map shows the area of New Zealand affected by earthquake-induced landslides triggered by the M_W 7.8 2016 Kaikoura Earthquake. 4

Figure 2.2 View looking west of the Hapuku rock avalanche and dam. The source area is outlined by a red dashed line. 5

Figure 2.3 Difference (ground-surface change) model for the Hapuku rock avalanche. 6

Figure 2.4 View of the Hapuku rock avalanche from the upstream side of the dam. Photo taken March 2017. 6

Figure 2.5 The Seafront rock slide/slump. The landslide source area outline is shown as a red dashed line. Note the debris flows sourcing from the toe of the debris. Photo taken December 2016. 7

Figure 2.6 Difference (ground-surface change) model for the Seafront rock slide/slump. 8

Figure 2.7 The Leader rock slide/slump. Note the main landslide dam (upper left) has breached and flow of water (the Leader River) has re-established. Photo taken in April 2017. 9

Figure 2.8 Difference (ground-surface change) model for the Leader rock slide/slump, draped over a three-dimensional topographic model. 9

Figure 2.9 Typical debris avalanches triggered by the earthquake on the slopes on the Inland and Seaward Kaikoura Ranges. 10

Figure 2.10 One of the many large-scale failures of coastal cliffs (Ohau Point, north of Kaikoura township), which inundated State Highway 1. 11

Figure 2.11 Landslide source area distribution for landslides triggered by the Kaikoura Earthquake and other significant earthquakes in New Zealand. 12

Figure 2.12 Landslide point and area density (N=10,195 landslides) within each 200 m distance from fault buffer. 13

Figure 2.13 Landslide source areas (N=10,195 landslides) normalised relative to the largest mapped landslide (area in km^2) and their associated elevation and slope angle taken from the 8 m resolution New Zealand digital elevation model. 14
Figure 2.14 The landslide dams triggered by the M_W 7.8 14 November 2016 Kaikoura Earthquake. 15
Figure 2.15 Landslide dam on the Conway River in greywacke. Photograph taken December 2016. 16
Figure 2.16 Landslide dam on the Hapuku River in greywacke. Photo taken December 2016. 16
Figure 2.17 A) Landslide dam on Ote Makura Stream (upstream from Goose Bay) in greywacke. B) Another view of the dam on the Conway River in greywacke. C) Landslide dam on the Medway River in sandstone and siltstone. D) Landslide dam on the Linton River in greywacke. E) Landslide dam on the Gelt River in greywacke. All photos taken in December 2016. 17
Figure 2.18 Landslide dam probability calculated from the data presented by Tacconi et al. (2016) and Korup (2004). 18
Figure 2.19 Hapuku River landslide and dam site-specific assessment results: 20
Figure 2.20 Point cloud from the ground based terrestrial laser scan (TLS) surveys of the Hapuku dam, looking upstream, vegetation is shown as green. Survey carried out in December 2016. 21
Figure 2.21 Coloured point cloud from the ground based terrestrial laser scan surveys of the Hapuku River dam, looking upstream from October 2017, after it had overtopped and breached. 21
Figure 2.22 University of Auckland students sieving landslide debris from the Hapuku River landslide dam after it breached in October 2017. 22
Figure 2.23 Landslide dam-breach debris flow/flood simulation for the Hapuku River landslide dam derived from numerical modelling. 22

TABLES

Table 3.1 Third party use of data generated by this research. 24
Table 3.2 Summary of reports, papers, theses that have used/relied on either funding, or collected information funded by, the emergency post Kaikoura Earthquake, NHRP funded project: Landslide inventory and landslide dam assessments 25

APPENDICES

A1.0 APPENDIX 1 – AIRBORNE LIDAR DATA 33
A2.0 APPENDIX 2 – METHODOLOGY FOR LANDSLIDE INVENTORY MAPPING 35
A2.1 Landslide inventory mapping team 35
A2.2 Objective of the landslide inventory: 35
A2.2.1 Value of the dataset 35
A2.3 Data capture and availability 36
A2.4 Data sources 36
A2.4.1 The initial inventory 36
A2.4.2 Revising the initial inventory 37
A2.5 Methodology (workflow) 37
A2.5.1 Landslide inventory geodatabase 37
A2.5.2 Landslide information being collected: 37

A3.0 APPENDIX 3 - SUMMARY OF DATA USED TO COMPILE THE LANDSLIDE INVENTORY 41

A4.0 APPENDIX 4 - LANDSLIDE DAM ASSESSMENT METHODS 44

A4.1 Regional-scale assessments 44

A4.2 Site-specific assessments 45

APPENDIX FIGURES

Figure A4.1 Landslide dam volume divided by dam height plotted against the area of the upstream catchment for each landslide dam included in the Korup (2004) and Tacconi et al. (2016) datasets. 45

APPENDIX TABLES

Table A2.1 Landslide source area attributes 38

Table A2.1 Continued 39

Table A2.1 Continued 39

Table A3.1 Summary of data used to compile the landslide inventory. 42

ABSTRACT

The M_W 7.8 14 November 2016 Kaikoura Earthquake generated more than 20,000 mapped landslides and about 200 significant landslide dams. Besides the immediate hazard from the landslides, cracked ground, landslide debris and landslide dams also pose longer-term risk to infrastructure, because if the landslides and debris remobilise and the dams breach, they could generate future debris flows and floods. These in turn, could sever transport routes and further damage infrastructure, adversely impacting the post-earthquake economic recovery of the region.

The goal of this short-term project was to collect perishable (ephemeral) data on landslides and landslide dams generated by the earthquake. Currently there are more than 20,000 landslide source areas in the landslide inventory.

Key findings from the landslide inventory are: 1) the number of large landslides (with source areas ≥10,000 m^2) triggered by the Kaikoura Earthquake is fewer than the number of similar sized landslides triggered by other similar magnitude earthquakes in New Zealand; 2) the largest landslides (with volumes from 5 to 20 M m^3) occurred either on or within 2,500 m of the 24 mapped faults that ruptured to the surface; and 3) the landslide density within 2,500 m of a mapped surface fault rupture is as much as three times higher than those densities farther than 2,500 m from a ruptured fault.

Around 200 significant landslide dams generated by the earthquake have now been mapped and combined with data from past New Zealand and overseas landslide dams. These data have been used to develop a regional-scale, empirically-based tool to assess the post-formation likelihood of dam failure (breaching), which can be used for future landslide dam generating events. Many of the larger dams have also been investigated in detail and dam-breach models have been calibrated from back-analysing their failure.

KEYWORDS

Earthquake-induced landslides, landslide dams, landslide hazard, landslide risk.

1.0 INTRODUCTION

The M_W 7.8 2016 Kaikoura Earthquake generated more than 20,000 mapped landslides and over 200 significant landslide dams. Some of these posed an immediate risk to people: The Goose Bay dam resulted in evacuation of residents from 29 homes, the Linton dam was situated upstream of a primary school and State Highway (SH) 70 road bridge, and the Hapuku dam is situated upstream of several homes and SH 1 road and rail bridge. The cracked ground, landslide debris and landslide dams also pose longer term risk to infrastructure, because if the landslides and debris remobilise and the dams breach, they could generate future debris flows and floods. These in turn could sever transport routes and further damage bridges, adversely impacting on economic recovery for the region.

The goal of this short-term project was to collect perishable (ephemeral) data on landslides and landslide dams generated by the earthquake. The landslides and other ground deformation hazards triggered by this earthquake differ from those triggered by the 2010/11 Canterbury earthquake sequence (e.g. Massey et al., 2014) and in other previous large earthquakes in New Zealand. The landslide inventories developed for this earthquake will compliment those collated from past New Zealand and international earthquakes, and will therefore add to, and compliment the international "body of knowledge" relating to earthquake-induced landslides (EIL). Such data is also fundamental for forecasting landslide severity in future earthquakes, as such forecast models need to be "trained" on high-quality EIL inventories.

The funding provided for this short-term project allowed us to "fill the gap" (a period of about a year) between the end of the work carried out for immediate post-earthquake response activities, and the start of other studies such as the five-year MBIE Endeavour PROP-52007-ENDRP-GNS Earthquake Induced Landscape Dynamics (EILD) programme[1]. Without this short-term funding, much of the perishable data would have been lost, jeopardising the utility of future research into landscape response to earthquakes.

The key tasks undertaken by this short-term research project were:

1. Complete mapping the landslide distribution triggered by the earthquake;
2. Carry out field-based landslide and landslide dam surveys and investigations, targeting specific sites of interest;
3. Compile data into a definitive landslide inventory and provide to stakeholders involved with the recovery;
4. Carry out regional-scale landslide dam assessments, and dam-specific breach modelling;
5. For selected dam sites, install monitoring equipment. This work was not carried out under this short-term project, as monitoring of the dams was carried out by the New Zealand Transport Agency (NZTA) and Environment Canterbury (ECAN).

To map the landslide and landslide dam distributions, we have primarily used post-earthquake 0.3 m ground resolution orthorectified aerial photographs, and digital surface models derived from them, alongside digital elevation models from post-earthquake airborne Light Detection and Ranging[1] (lidar) surveys, and other pre- and post- Kaikoura Earthquake imagery and lidar data.

[1] Lidar is a surveying method that measures distances using a laser. The data used in this project was collected from an aeroplane at various times after the earthquake, and made into high resolution topographic models.

Lidar data was critically important for the mapping of landslides and site-specific landslide dam surveys and assessments (Appendix 1).

Landslides were manually digitised directly into a Geographic Information System (GIS). We also relied on the geotagged oblique air photos taken from multiple post-earthquake helicopter reconnaissance missions to support and verify mapping in areas of complex terrain. The landslide mapping was carried out by experienced landslide researchers using the scheme outlined by Dellow et al. (2017a) and contained in Appendix 2. The datasets used to map the landslide distribution are summarised in Appendix 3.

2.0 KEY FINDINGS

2.1 Landslide inventory mapping

The distribution of landslides triggered by the Kaikoura Earthquake has been mapped sequentially over time, with mapping starting in the days immediately after the earthquake. The area affected by landslides is approximately 10,000 km^2, and mapping such a large area takes time. To ensure that the agencies responsible for the earthquake response and recovery had the data they needed in a timely manner, we decided during the response phase (in the first few months after the earthquake), to distribute the mapped inventory sequentially, to the agencies who needed it. Updates were sent weekly during the response phase, and monthly during the recovery phase.

This short-term project allowed the mapping to continue after the response phase, culminating in the release of Version 1.0 of the landslide inventory in August 2017 (Figure 2.1). The Version 1.0 landslide inventory contains 10,195 EIL and is presented in Massey et al. (2018). The version 1.0 inventory contains the results from mapping most of the larger landslides triggered by the earthquake, present in the entire area affected by landslides. It includes some landslides contained in preliminary inventories, mapped from low-resolution satellite images, presented by Rathje et al. (2016). The Version 1.0 inventory is therefore relatively complete for the entire area affected, for those landslides typically > 5,000 m^2. It is version 1.0, because:

1. mapping was ongoing at the time Massey et al. (2018) was published, in those areas where the landslide distribution was initially mapped from satellite images; and,
2. although many smaller landslides (<5,000 m^2) are included in the Version 1.0 inventory, they had not all been mapped at the time of publication, in part due to the delay in receiving the higher resolution aerial photographs and lidar data.

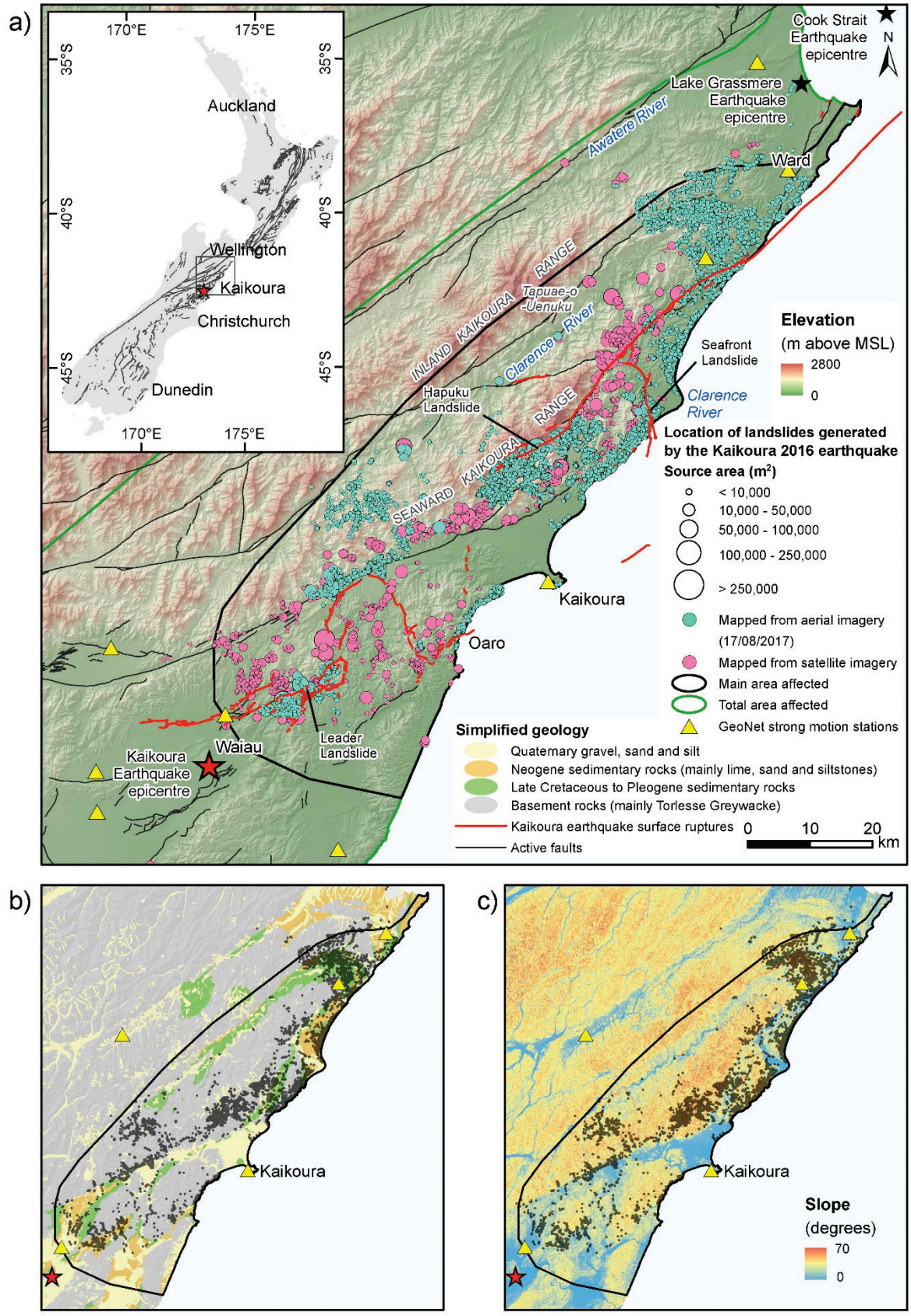

Figure 2.1 Inset map shows the area of New Zealand affected by earthquake-induced landslides triggered by the M_W 7.8 2016 Kaikoura Earthquake. a) The mapped Version 1.0 of the mapped 10,195 EIL source areas and their size (area) triggered by the earthquake, superimposed on the 8 m ground resolution digital elevation model for New Zealand, classified by elevation in meters above sea level and hill-shaded from the northwest. b) The landslide source area distribution overlain on the main geological units (after Heron, 2014). c) Landslide source area distribution shown on the 8 m ground resolution digital elevation model for New Zealand.

2.1.1 Examples of landslides triggered by the earthquake

Several types of landslide were triggered by the earthquake.

The Hapuku rock avalanche in Lower Cretaceous basement rocks (greywacke) (Figure 2.2) is the largest of the mapped landslides, with an estimated volume of about 20 (±2) M m^3. In this case, the slide surface appears to correspond to multiple persistent discontinuities such as old and recent fault planes. Several faults that ruptured to the surface in the Kaikoura Earthquake (Litchfield et al. 2018; Nicol et al. 2018) pass through the source area of the landslide. The debris left the source and blocked the Hapuku River creating a dam about 100 m high (Figure 2.3). Multiple lobes of debris of different clast size are visible in the deposit, indicating multiple pulses of debris deposition (Figure 2.4). The dam overtopped and the downstream face was partially eroded (due to headward erosion initiated by seepage through the dam) following Cyclone Cook in April 2017. The debris left in the source is still unstable and several debris flows have occurred, which have eroded the debris down to bedrock in places. The debris forming the dam continues to erode as water from the impounded lake flows over the crest and down the outflow channel.

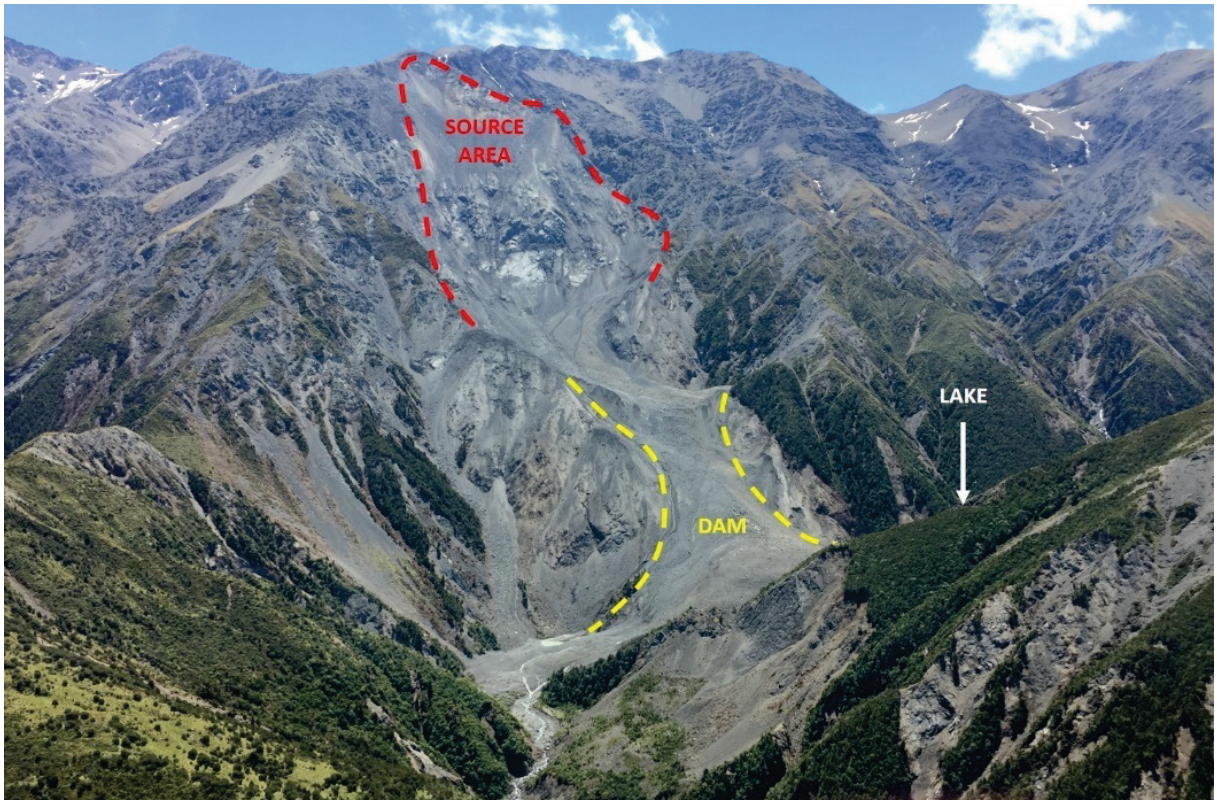

Figure 2.2 View looking west of the Hapuku rock avalanche and dam. The source area is outlined by a red dashed line. The extent of the debris is outlined by a yellow dashed line. The impounded lake (obscured) and location of the dam are labelled. The dam overtopped on 6 April 2017 and eroded about 2 m off the dam outlet. The dam again overtopped and a substantial breach occurred in October 2017 following rain. Photo taken December 2016.

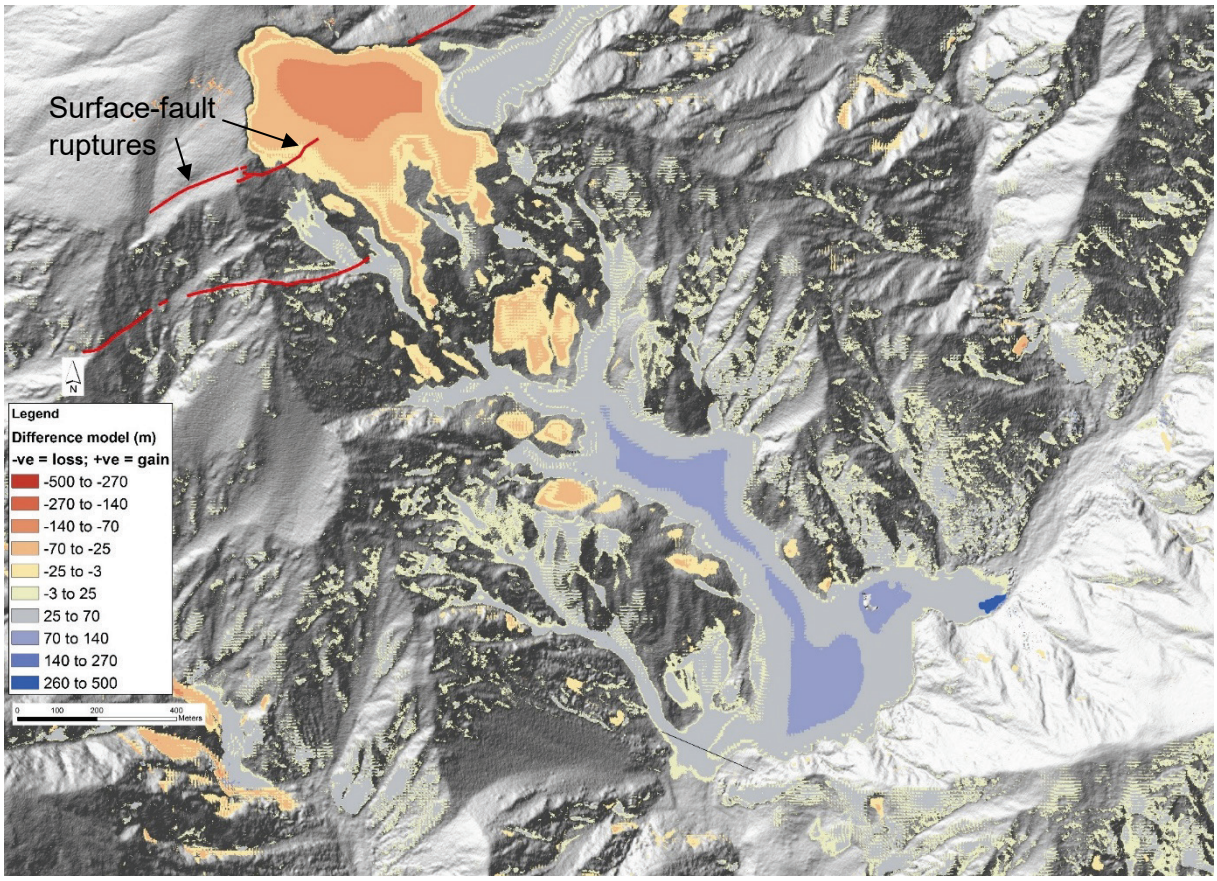

Figure 2.3 Difference (ground-surface change) model for the Hapuku rock avalanche. The difference model was developed by subtracting the pre-earthquake digital surface model (DSM) developed from the 0.3 m resolution aerial images, from the post-earthquake surface model derived from airborne lidar. The difference model does not show any vertical changes (positive or negative) of less than ±3 m, as these smaller changes mostly represent vegetation effects. Reds, oranges and yellows represent loss of material inferred to be erosion. Blues to purples represent a gain of material inferred to be deposition. Red lines represent faults that ruptured to the surface.

Figure 2.4 View of the Hapuku rock avalanche from the upstream side of the dam. Photo taken March 2017.

The Seafront rock slide/slump in Paleogene limestone (Figure 2.5) is the largest mapped landslide in these materials with an approximate volume of 10 (±2) M m^3. The slide surface is assumed to be deep seated (>100 m below the surface in places), with the field observations and cross sections suggesting a semi-rotational failure through the rock mass. Much of the debris has remained intact, and so the slide/slump would be classified as coherent (Keefer, 2013). The displaced mass is still creeping and several debris flows have occurred both off the toe of the intact displaced debris and the head scarp. The Papatea fault (Hamling et al., 2017; Litchfield et al., 2018; Langridge et al., 2018) ruptured through the source area suggesting that surface rupture of this fault caused the landslide to initiate (Figure 2.6). We are not sure whether the landslide initiated either from permanent earthquake-induced displacement of the ground or dynamic displacement caused by shaking, or some combination of both. The ground-surface change model (difference model) (Figure 2.6), indicates that much of the landslide debris remained intact and within the source area, and the displacement vectors of the debris indicate a rotational movement mechnism.

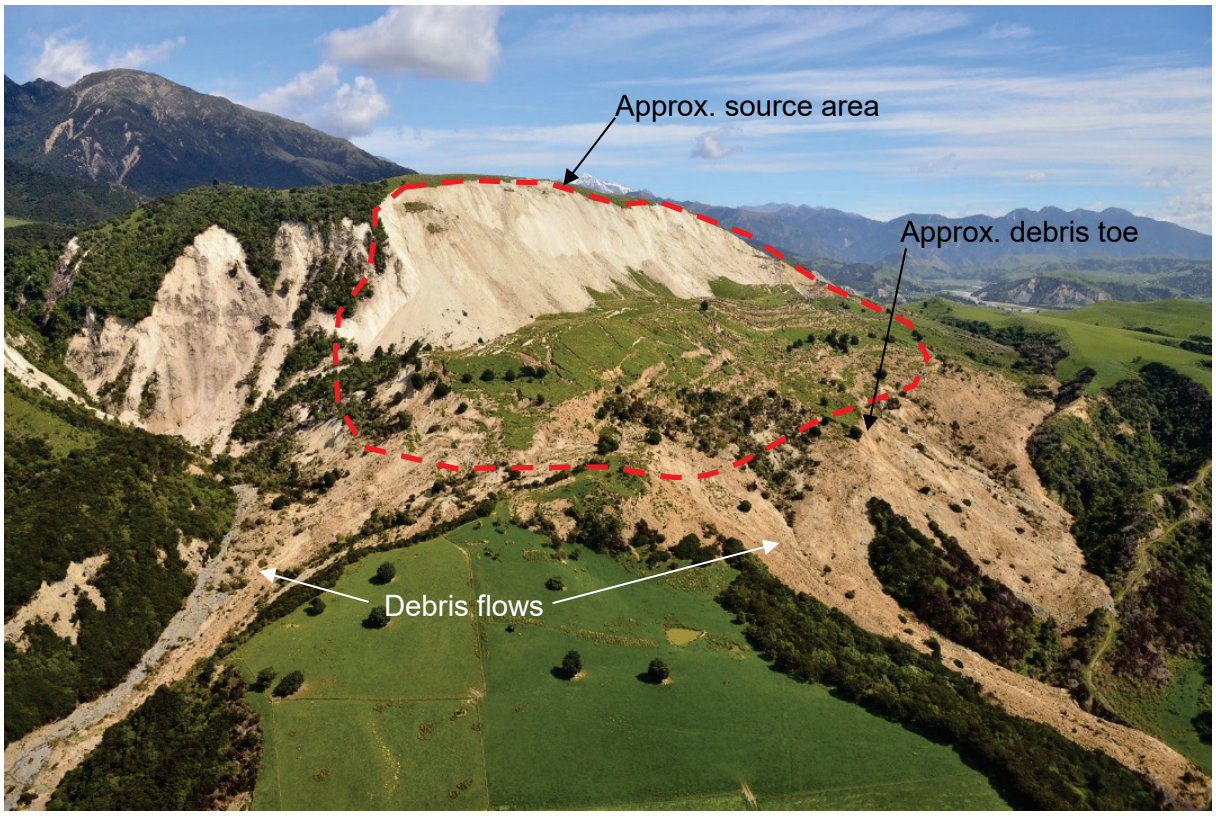

Figure 2.5 The Seafront rock slide/slump. The landslide source area outline is shown as a red dashed line. Note the debris flows sourcing from the toe of the debris. Photo taken December 2016.

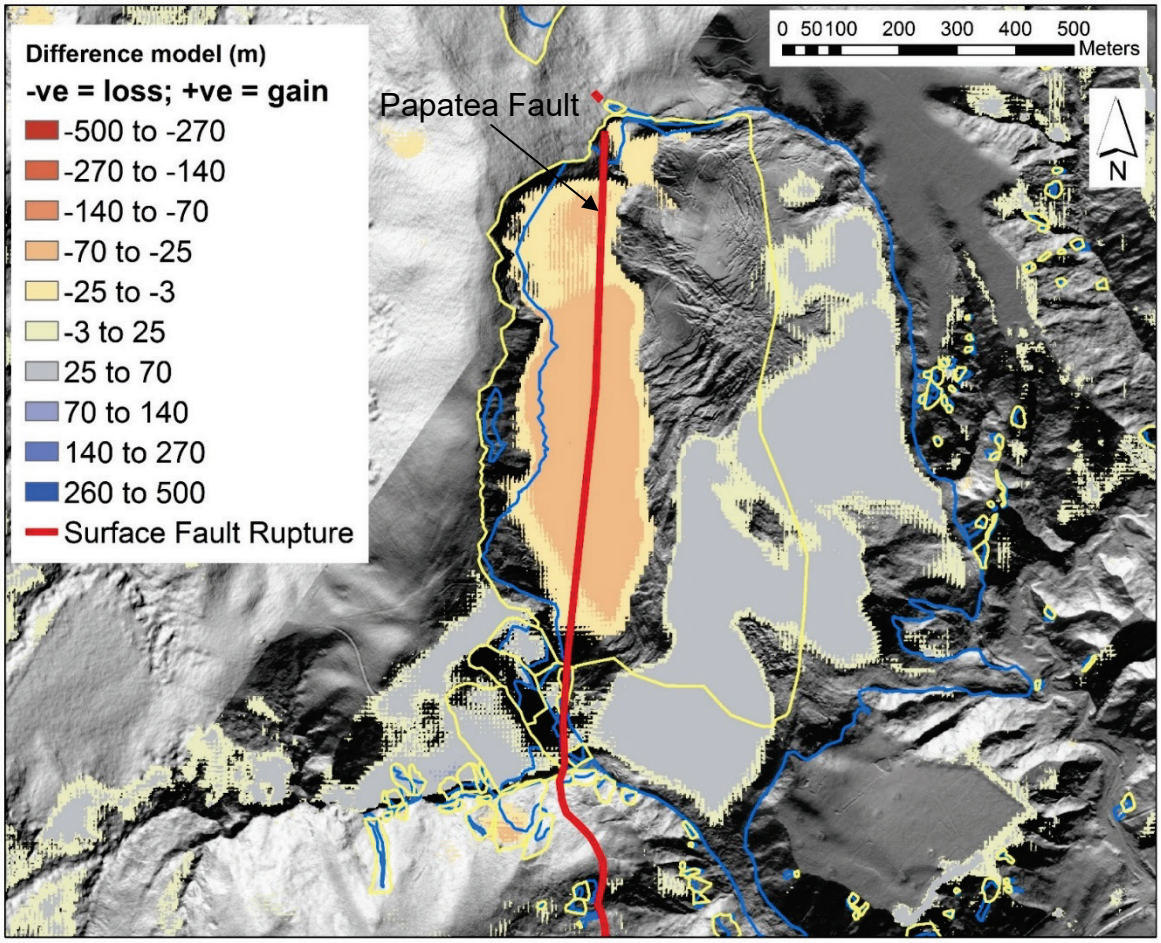

Figure 2.6 Difference (ground-surface change) model for the Seafront rock slide/slump. The difference model was developed by subtracting the pre-earthquake digital surface model (DSM) developed from the 0.3 m resolution aerial images, from the post-earthquake surface model derived from airborne lidar. The difference model shown does not show any vertical (positive or negative) changes of less than ±3 m. Reds, oranges and yellows represent loss of material inferred to be erosion. Blues to purples represent a gain of material inferred to be deposition.

The Leader River rock slide/slump in Neogene mudstone (Figure 2.7) is the largest mapped landslide in these materials with an approximate volume of 6 (±1) M m^3. The slide surface is assumed to be deep seated (about 80 m below the surface in places) with the difference model (Figure 2.8) indicating that much of the debris moved as intact blocks. The displacement vectors of the debris suggest a translational failure (with some rotation at the head scarp), possibly along bedding. A faulted contact between the Lower Cretaceous greywacke and Neogene mudstone is exposed in the northern end of the landslide head scarp. Although there is no field-evidence to suggest this fault ruptured (Nicol et al., 2018), it is possible that some fault ruptured through the source area (head scarp) of this landslide. More investigation is needed to determine whether this is the case or not.

Figure 2.7 The Leader rock slide/slump. Note the main landslide dam (upper left) has breached and flow of water (the Leader River) has re-established. Photo taken in April 2017.

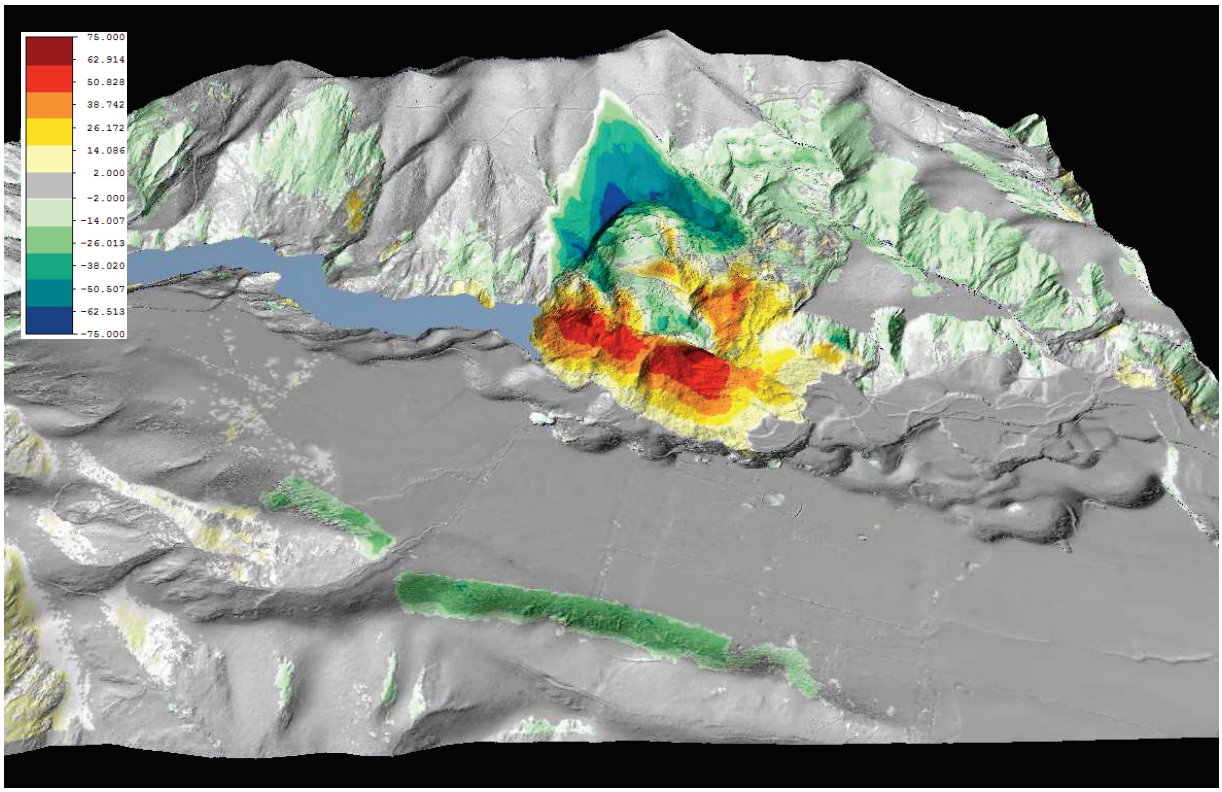

Figure 2.8 Difference (ground-surface change) model for the Leader rock slide/slump, draped over a three-dimensional topographic model. The difference model was developed by subtracting the pre-earthquake digital surface model (DSM) developed from the 0.3 m resolution aerial images, from the post-earthquake surface model derived from airborne lidar. The difference model does not show any vertical (positive or negative) changes of less than ±2 m. Blues to greens represent loss of material inferred to be erosion. Reds, oranges and yellows represent a gain of material inferred to be deposition.

Many smaller landslides were also triggered across an area of about 10,000 km^2, with most being concentrated within an area of about 3,600 m^2 (Figure 2.1). Many comprised debris avalanches, the most notable being those along the coast north and south of Kaikoura (Figure 2.9). The landslides along the coast caused substantial damage to both State Highway (SH) 1 and the northern section of the South Island Main Trunk Railway (Figure 2.10), blocking both in multiple locations (Davies, 2017). It took more than a year to reopen both the road and rail after the earthquake, in part because of the challenges of removing the landslide debris.

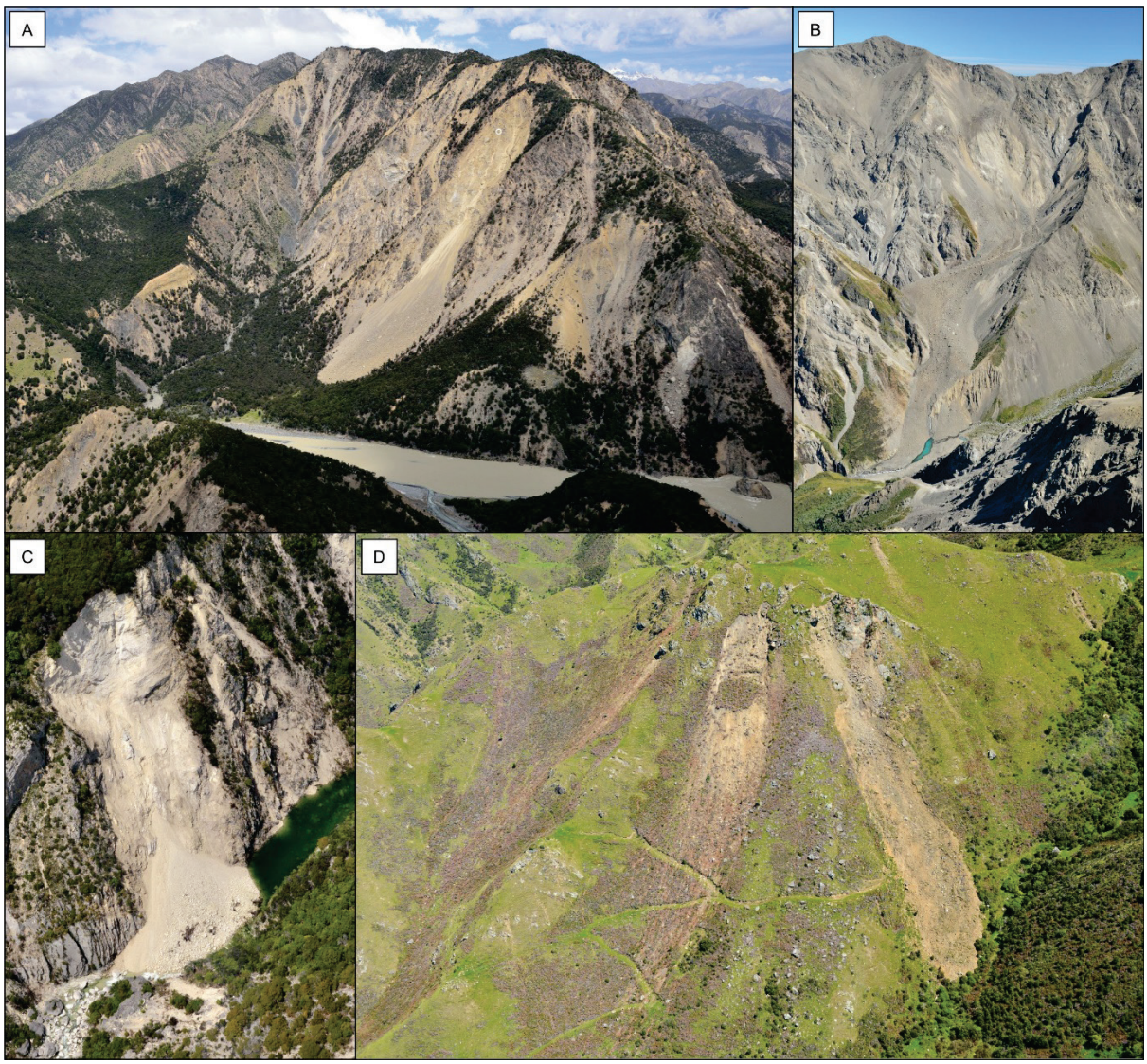

Figure 2.9 Typical debris avalanches triggered by the earthquake on the slopes on the Inland and Seaward Kaikoura Ranges. A: Clarence valley; B Kowhai headwaters; C: Waima River; D: Flaxbourne hills.

Figure 2.10 One of the many large-scale failures of coastal cliffs (Ohau Point, north of Kaikoura township), which inundated State Highway 1. At this location, the South Island Main Trunk Railway is within a tunnel through the headland.

2.1.2 Preliminary analysis of landslide inventory results

Massey et al. (2018) used Version 1.0 of the landslide inventory to identify and discuss some of the controls on the spatial distribution of landslides triggered by the Kaikoura Earthquake. The key findings from Massey et al. (2018) are:

1. the number of large landslides (with source areas ≥10,000 m^2) triggered by the Kaikoura Earthquake is fewer than the number of similar sized landslides triggered by other similar magnitude earthquakes in New Zealand (Figure 2.11);
2. the largest landslides (with source volumes from 5 to 20 M m^3) occurred either on or within 2,500 m of the 24 mapped faults (Litchfield et al., 2018) that ruptured to the surface (Litchfield et al., 2018);
3. the landslide density within 2,500 m of a mapped surface fault rupture is as much as three times higher than those densities farther than 2,500 m from a ruptured fault;
4. for the same slope angles, coastal slopes have landslide point densities that are an order of magnitude greater than those in similar materials on the inland slopes, but their source areas are significantly smaller. This possibly indicates that the coastal slopes locally amplified ground shaking, and
5. Most landslides occurred within 2,500 m of a fault rupture that ruptured to the surface. Such a relationship could be used as a proxy for ground-motion intensity, i.e. typically stronger shaking occurs closer to a fault that ruptures. This relationship might be because the distance to fault captures:
    a. the high-frequency ground motions and their attenuation with distance from a fault better than the current earthquake ground-motion models;

b. the complexity of the multi-fault rupture, and therefore the multi-frequency ground motion intensity; and

c. the more damaged nature of the rock masses close to the faults, where they tend to be more sheared and weakened by previous fault displacements. The strong relationship between the "distance to fault" and the landslide distribution could also reflect the apparent structural control (i.e., fault surface rupture) of some of the largest landslides that occur on or near faults.

We have estimated a preliminary total volume of all landslides triggered by the Kaikoura Earthquake from surface difference models. This was done for a selection of landslide-affected areas, by subtracting pre- and post-earthquake digital topographic surface models derived from air photos and lidar data. In these areas we established landslide source area to volume ratios, which we then used to estimate the range of landslide source volumes, for those mapped landslide source areas in the Version 1.0 inventory. The total volume is estimated to range between 100 and 200 M m^3. The broad range is due to the uncertainties associated with: 1) estimating volumes for those landslides where debris remains in the source area; and 2) the landslide source area to volume ratios used.

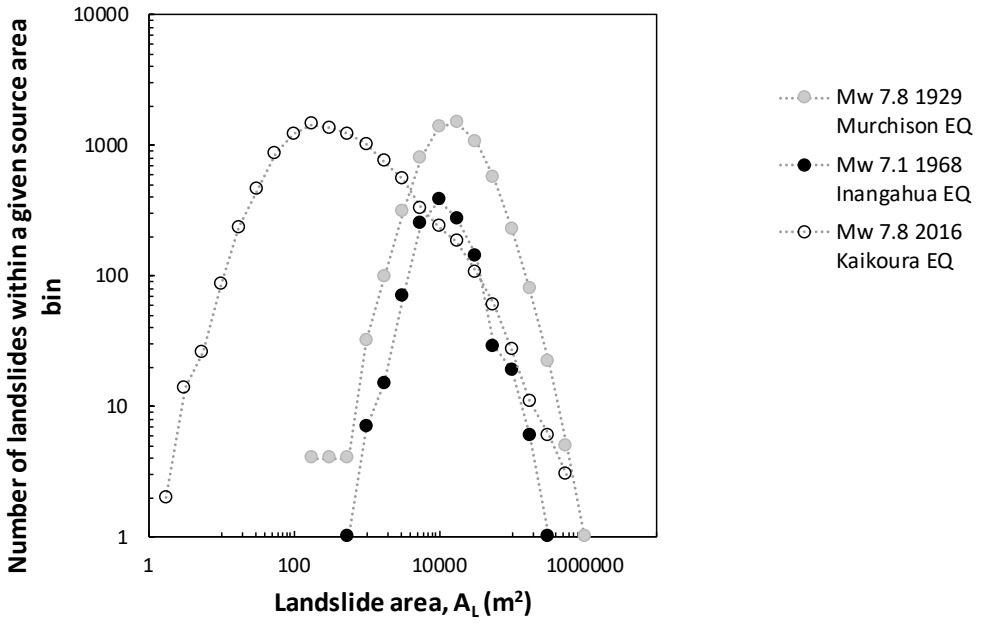

Figure 2.11 Landslide source area distribution for landslides triggered by the Kaikoura Earthquake and other significant earthquakes in New Zealand. The number of landslides (frequency) with source areas within each source area bin. The figure plots landslides generated by the Kaikoura Earthquake, the M_W 7.1 1968 Inangahua, New Zealand earthquake (Hancox et al., 2014) and the M_W 7.8 1929 Murchison, New Zealand earthquake (Hancox et al., 2016).

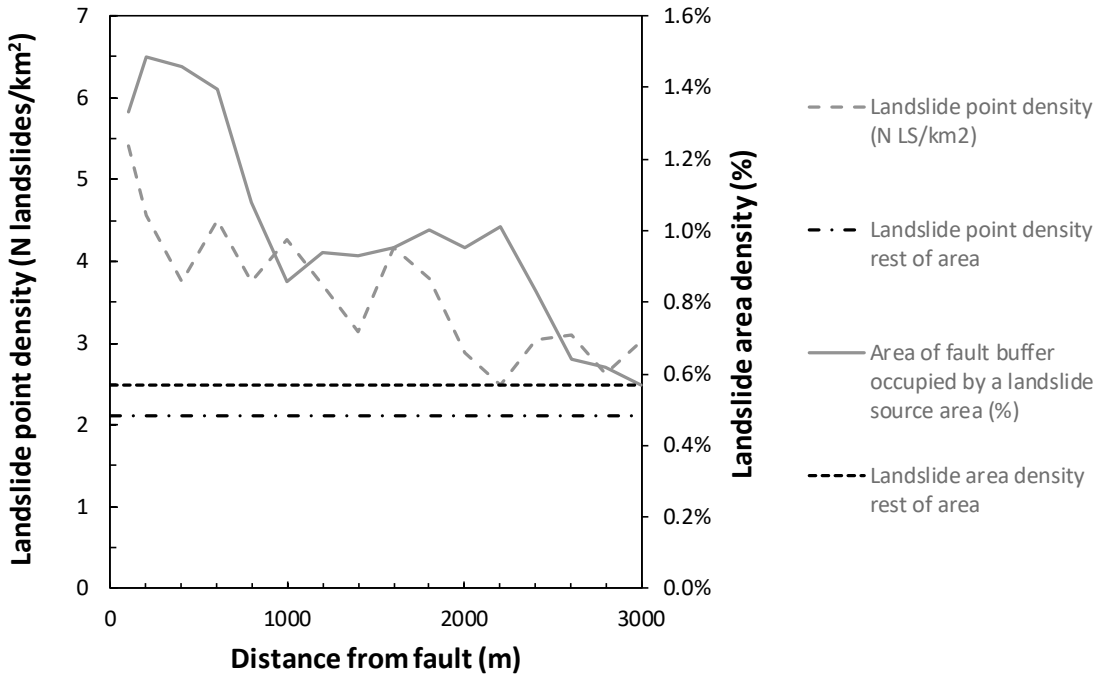

Figure 2.12 Landslide point and area density (N=10,195 landslides) within each 200 m distance from fault buffer. Landslide density is calculated by taking the centroid of each landslide source area that falls within each 200 m distance buffer from the mapped surface expression of the faults that ruptured during the earthquake. The number (N) of landslide points within each distance from fault bin range is then divided by the area of slope (km^2) within each bin. The landslide area density is also shown, which is calculated in the same way as the landslide point density; however, the area of each landslide source (km^2) within each distance from fault bin is summed and divided by the total area of ground within each 200 m bin.

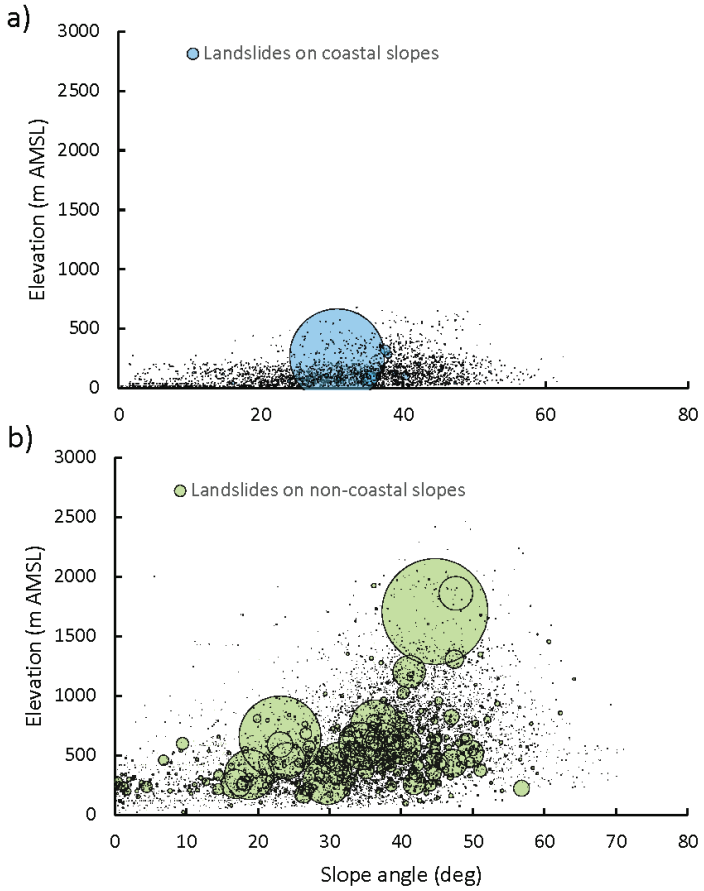

Figure 2.13 Landslide source areas (N=10,195 landslides) normalised relative to the largest mapped landslide (area in km^2) and their associated elevation and slope angle taken from the 8 m resolution New Zealand digital elevation model.

2.2 Landslide dams

Aerial (helicopter) reconnaissance flights, carried out in the first few days and weeks after the earthquake eventually identified 196 significant drainage blocking or drainage constricting landslides in the area affected by landslides (Figure 2.14) (Dellow et al., 2017b). Of concern was the debris flood and flow hazards that could result should some of the landslide dams breach catastrophically. Several of the dams were located upstream from people and critical infrastructure, such as road and rail bridges, which could potentially be at risk if a dam-breach and flood event were to occur.

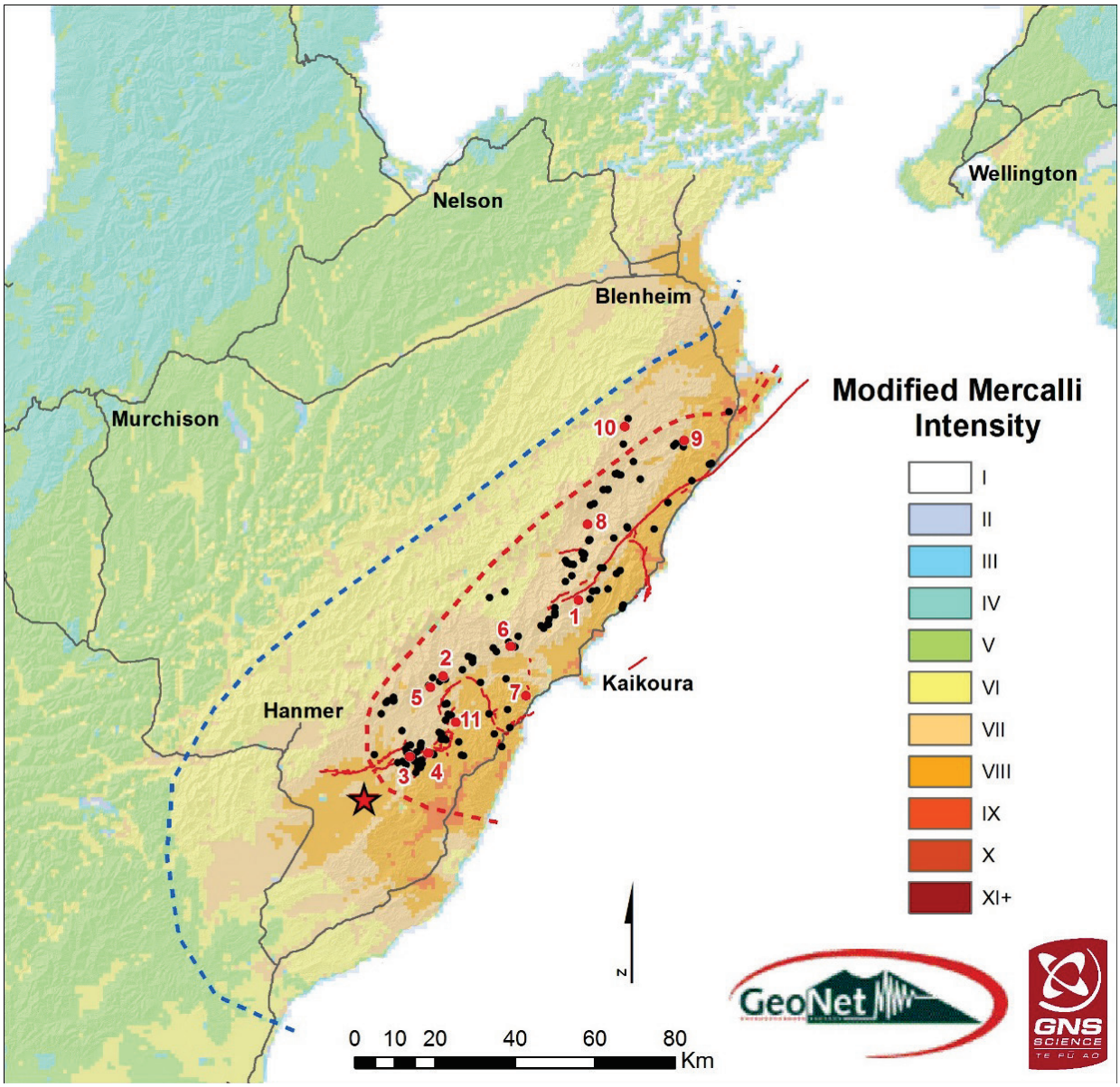

Figure 2.14 The landslide dams triggered by the M_W 7.8 14 November 2016 Kaikoura Earthquake. The epicentre is shown by the red star. The colours depict the MM (ground) Shaking Intensity, with MM VIII in the worst affected areas and isolated pockets of MM IX where deep soils are present. Areas of light to moderate landslide damage (area between the blue dashed and red dashed lines), and severe landslide damage (area inside the red dashed line) are also shown. Faults that ruptured to the ground surface are shown as solid red lines (Litchfield et al., 2018). The landslide dams are shown as black dots, or for the dams assessed having the highest failure hazard and consequential risks are numbered and shown by a red dot: 1: Hapuku; 2: Conway; 3: Stanton; 4. Leader; 5. Towy; 6. Linton; 7. Ote Makura (Goose Bay); 8. Clarence; 9. Waima/Ure; 10: Medway; 11. Gelt. (Map updated from Dellow et al., 2017b).

Each landslide dam and impounded lake varied in geometry and volume. Figure 2.15 to Figure **2.17** show examples of the dams generated in different source materials. Some dams, such as the main one on the Clarence River, breached within 24-hours of being formed, but most breached during rainstorms in March, April and October 2017. The only significant dam that remains is the one on the Hapuku River (Figure 2.16). This dam has partially failed via a combination of backward erosion on the downstream face and overtopping. Site-specific surveys pre- and post-breaching were carried out for the main landslide dams on the Hapuku, Linton, Conway, Towy, Stanton and Leader rivers and the Ote Makura Stream, where people and infrastructure were potentially at risk. These are discussed in the next section.

Figure 2.15 Landslide dam on the Conway River in greywacke. Photograph taken December 2016.

Figure 2.16 Landslide dam on the Hapuku River in greywacke. Photo taken December 2016.

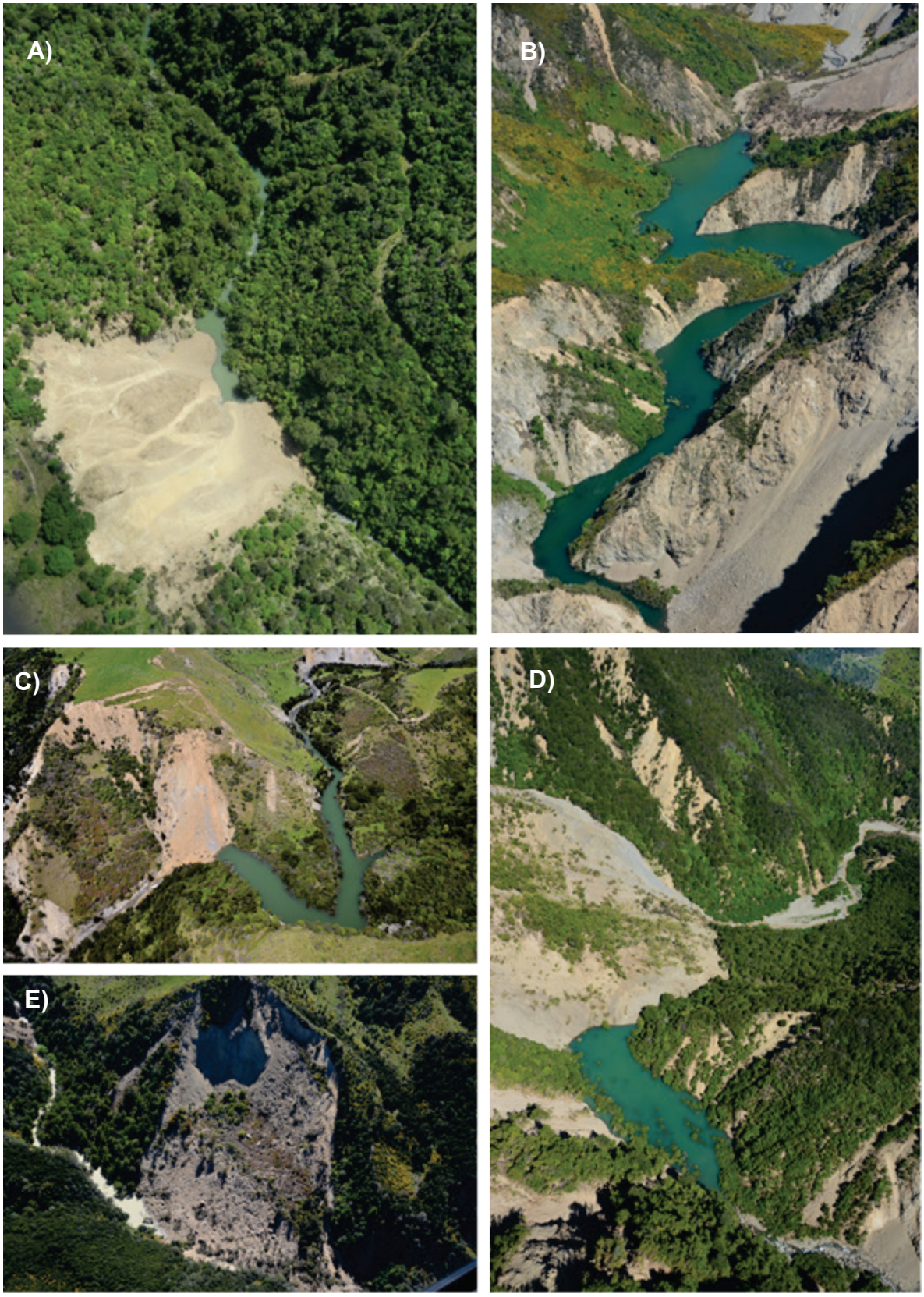

Figure 2.17 A) Landslide dam on Ote Makura Stream (upstream from Goose Bay) in greywacke. B) Another view of the dam on the Conway River in greywacke. C) Landslide dam on the Medway River in sandstone and siltstone. D) Landslide dam on the Linton River in greywacke. E) Landslide dam on the Gelt River in greywacke. All photos taken in December 2016.

2.2.1 Regional-scale landslide dam assessments

The methodology used to assess the likelihood of dam failure, adopting empirically-based models is detailed in Appendix 4. The key findings from this work are shown in Figure 2.18. The plot suggests that the main dam on the Clarence River was calculated to have a high probability of failure. This dam failed within 24-hours of being formed. Conversely, these data indicate that the dam on the Hapuku River has the lowest calculated probability of failure of the Kaikoura landslide dams plotted. These dams have now failed, most failed in the rain that occurred during Cyclones Cook and Debbie in March and April 2017, but the Hapuku dam is still present and poses a potential, albeit reduced risk, to people downstream.

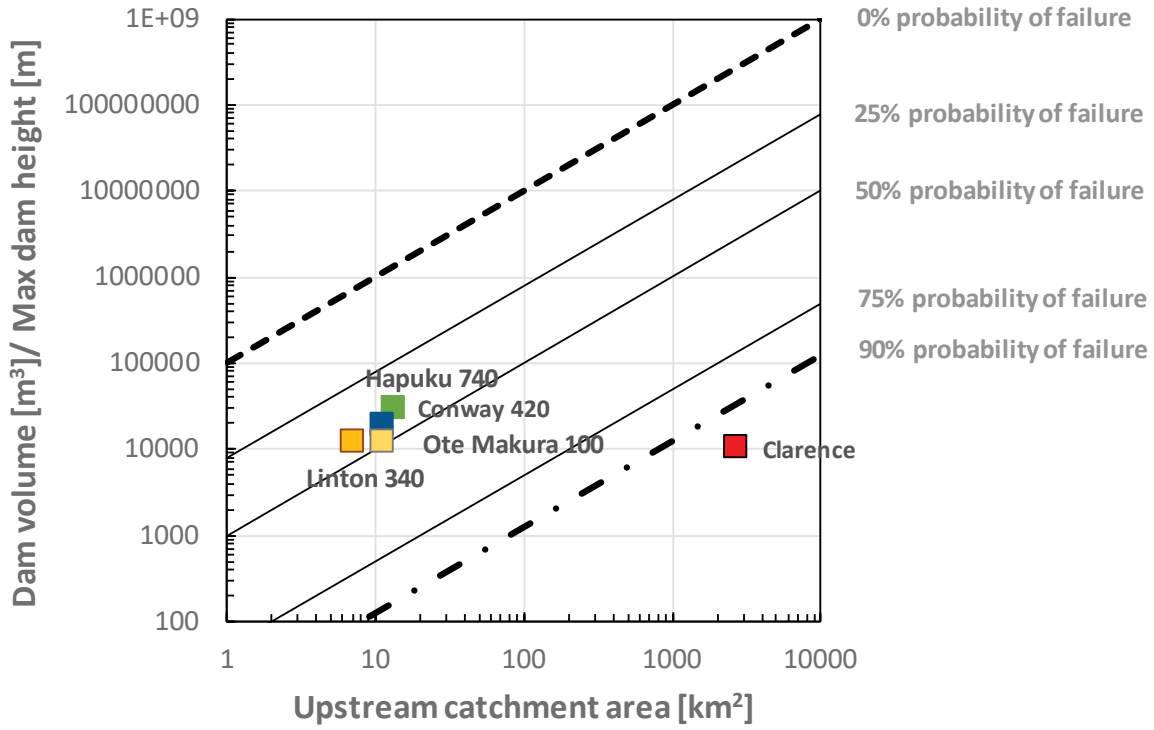

Figure 2.18 Landslide dam probability calculated from the data presented by Tacconi et al. (2016) and Korup (2004). The dam volumes and maximum (Max) dam heights and the upstream catchment areas calculated for the main landslide dams triggered by the Kaikoura Earthquake are plotted so that their probability of failure can be evaluated.

2.2.2 Site-specific landslide assessments

The site-specific assessments were carried out for seven of the larger dams where dam-breach hazards could potentially pose a downstream risk to people. These were carried out for the Hapuku, Linton, Conway, Towy, Stanton and Leader Rivers and the Ote Makura stream. Details of the assessments are contained in Appendix 4.

The key findings from this work are:

1. Airborne and ground based lidar surface models surveyed before and after the dams breached provided high-resolution models of their surfaces (Figure 2.19, Figure 2.20 and Figure 2.21). These surfaces were differenced (subtracted from one another) to generate surface change models and the dam details accurately measured, e.g., dam volume, geometry and impounded lake volumes and geometry. Detailed models of natural dams generated this way are rare, both in New Zealand and overseas. Such information is critical for assessing the stability and likely longevity of the dam on the landscape;

2. The dam dimensions were used to estimate the dimensionless blockage index (DBI), which is an empirically-based index used to assess dam stability. Most of the landslide dams generated by the Kaikoura Earthquake had DBI ≤3, indicating that they were likely to be unstable when compared to other natural dams in New Zealand (Korup, 2004) and overseas (Tacconi et al. 2016);
3. Field surveys of debris flows and floods and the particle size distribution (Figure 2.22) of the debris, generated by the breaches of the dams were used to calibrate the dam-breach debris-flood inundation forecast simulations (carried out before the dams breached) (Figure 2.23). These comparisons showed that many of the downstream consequences (in this case the debris inundation levels) were similar to the debris inundation levels, forecast by the simulations assuming the "most likely" conditions (Dellow et al., 2017). Therefore, the forecast models matched well what happened, and so are a useful method for assessing debris flood hazards in similar future events.

Further regional-scale and site-specific studies of the landslide dams are currently underway as part of the EILD programme.

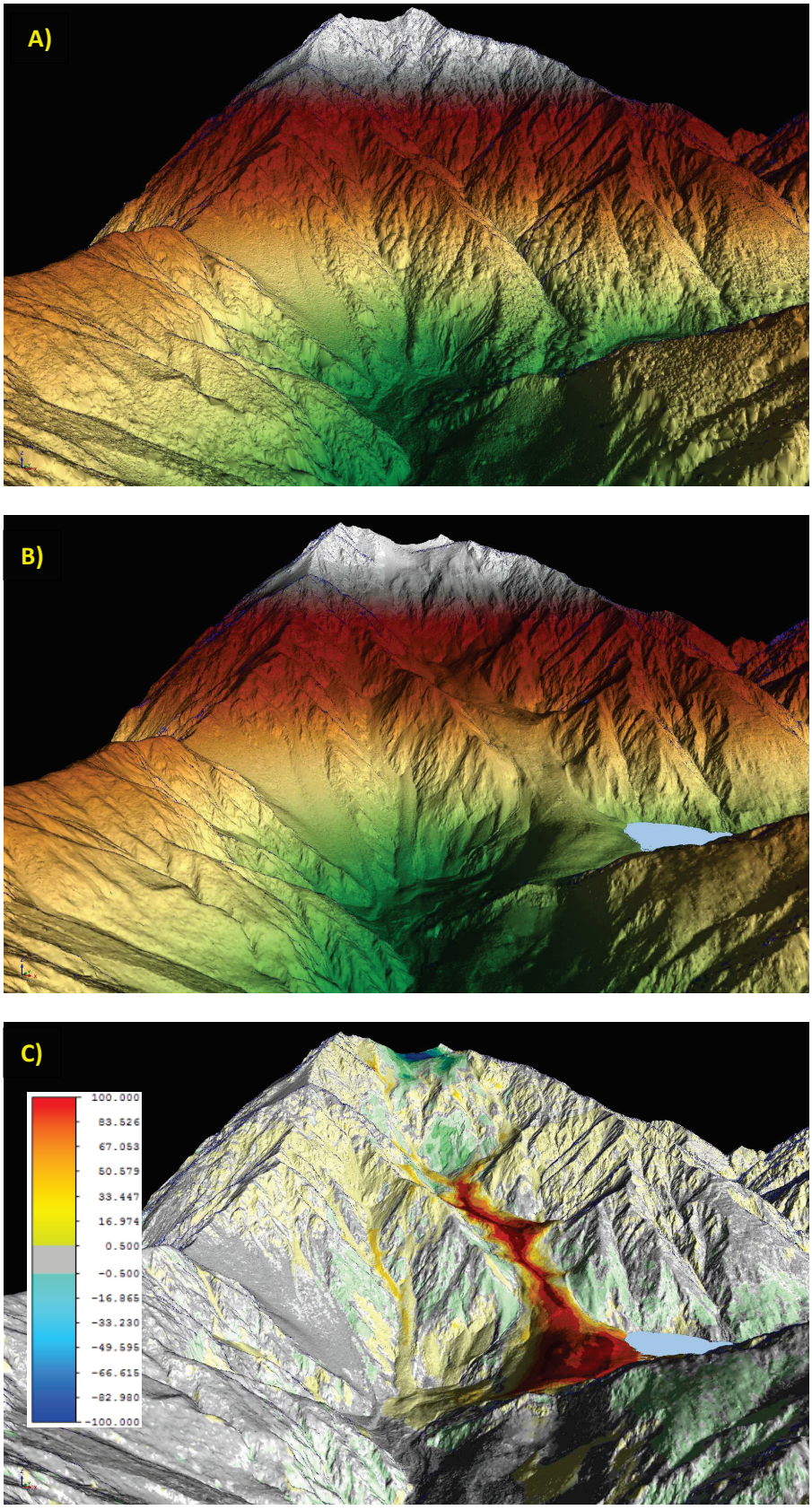

Figure 2.19 Hapuku River landslide and dam site-specific assessment results: A) pre-earthquake digital surface model of slopes derived from photogrammetry. B) Post-earthquake digital elevation model derived from airborne lidar. C) the difference between the two surface models, where warm colours are deposition of debris, and the cold colours are loss of material in the landslide source area. The lake impounded behind the dam is shown in light blue.

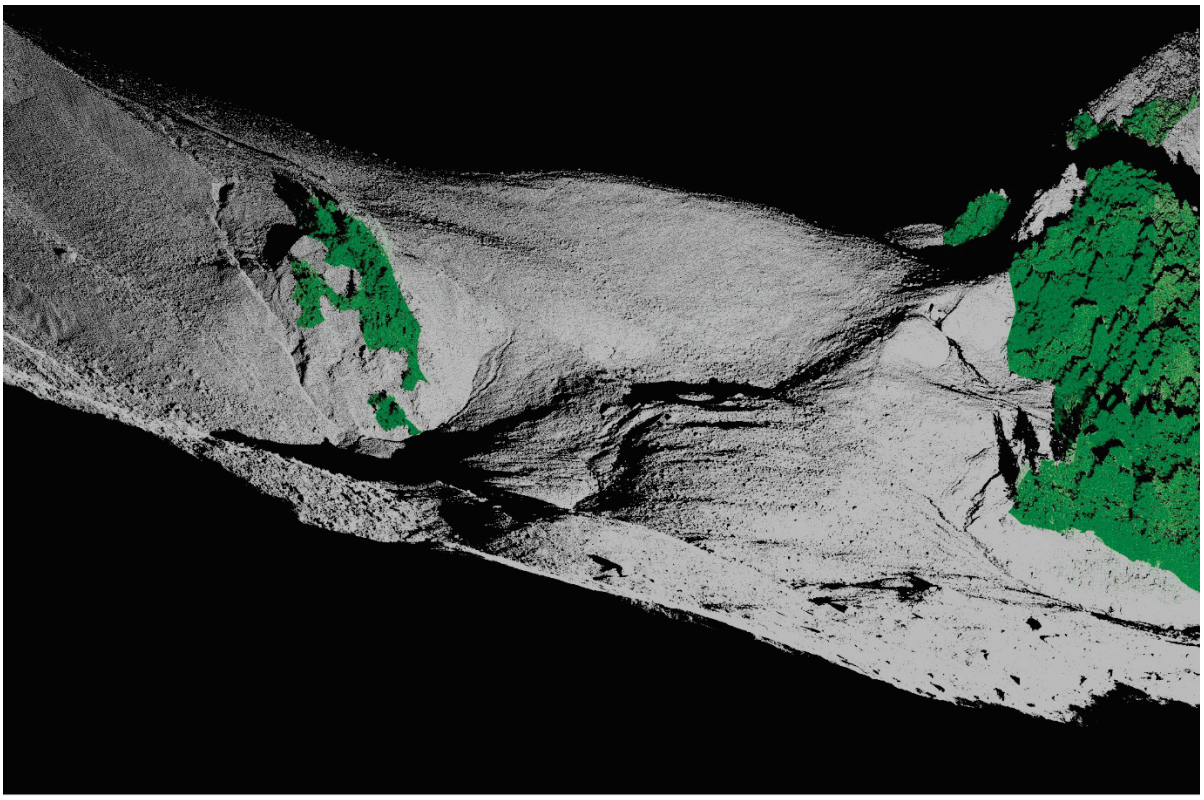

Figure 2.20 Point cloud from the ground based terrestrial laser scan (TLS) surveys of the Hapuku dam, looking upstream, vegetation is shown as green. Survey carried out in December 2016.

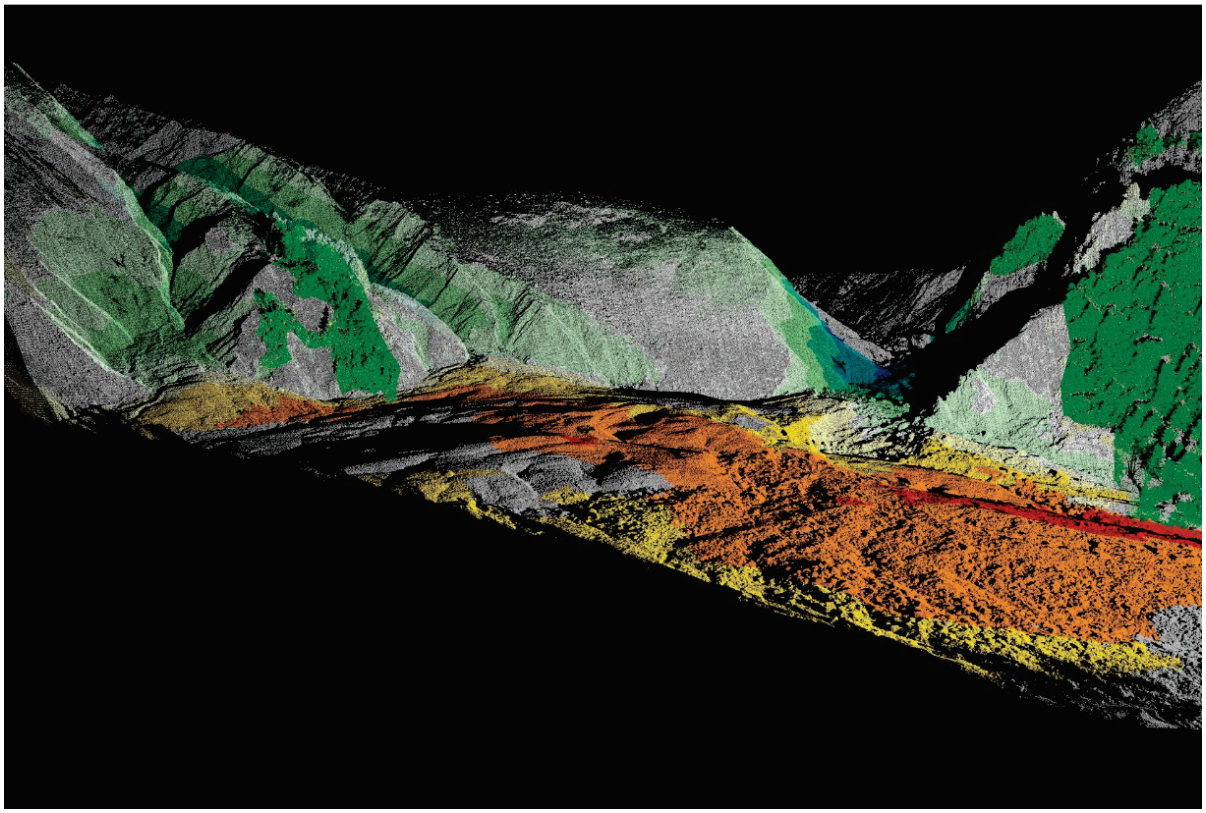

Figure 2.21 Coloured point cloud from the ground based terrestrial laser scan surveys of the Hapuku River dam, looking upstream from October 2017, after it had overtopped and breached. Note the breach geometry on the right of the lower image. The approximate volume of dam material eroded is about 1 M m^3. Much of the dam is still present, but water continues to flow out of the lake along the breach channel. The orange and red colours represent material deposition (aggradation) and the blues and greens represent material erosion.

Figure 2.22 University of Auckland students sieving landslide debris from the Hapuku River landslide dam after it breached in October 2017.

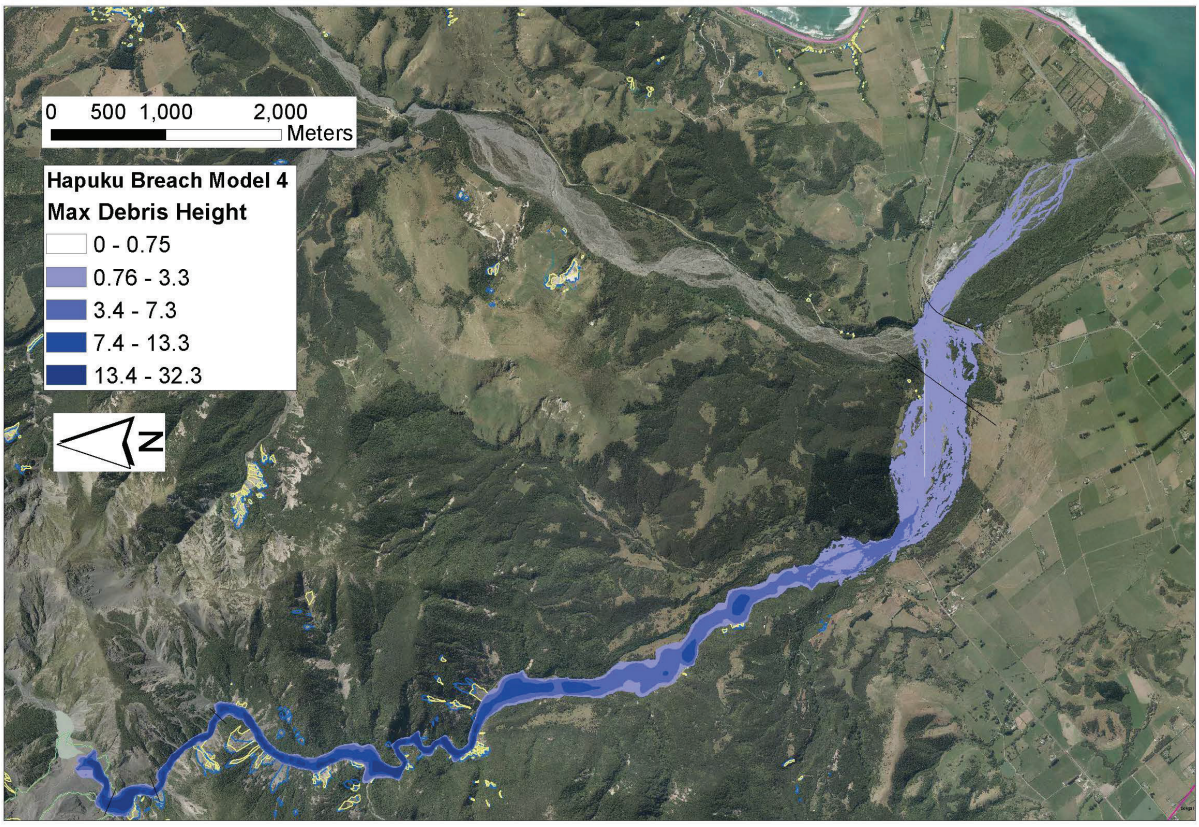

Figure 2.23 Landslide dam-breach debris flow/flood simulation for the Hapuku River landslide dam derived from numerical modelling. The model simulates the assumed "worst credible" event, based on the entire dam failing catastrophically. In October 2017, the dam overtopped and partially breached. Much of the material forming the dam remains, but the impounded lake level has dropped as a result erosion caused by water flowing through the breach channel.

3.0 DISCUSSION

3.1 Who has used the data

Table 3.1 details who has used the various datasets generated by this project and Table 3.2 is a summary of the reports, papers, theses that have used/relied either on funding, or collected information funded by this project.

Table 3.1 Third party use of data generated by this research.

Data generated by this research	Description of data	Entity requesting/using data
Landslide database	Digital geospatial outlines (polygons) of landslides assumed to have been triggered by the Kaikoura Earthquake, which were mapped as part of this research. The data is in GIS format. Landslide triggered by some of the more significant rain events, post-earthquake (e.g., ex tropical cyclone Gita) have also been mapped.	**Environment Canterbury (ECAN), Kaikoura District Council, Hurunui District Council and Marlborough District Council (MDC**), to identify urban and rural areas as well as sections of urban road (and other infrastructure) more severely affected by earthquake-induced landslides. Also used as an input to help with future planning. **Department of Conservation (DOC)**, to restrict access and/or warn users of the landslide hazards present in various locations on the DOC estate. **GNS Science**, as input for the "North Canterbury Transport Infrastructure Recovery (NCTIR) alliance – Pilot study for assessing landslide hazards along the road and rail corridors. **NCTIR**, as input for their recovery work for the road and rail corridors. **Engineering consultants** (OPUS, Aurecon, URS, T&T, Golder, EngGeo) for their recovery related work for the road and rail corridor, but also for individual house inspections. **NZTA and KiwiRail**, as part of their resilience study for the road and rail corridor. **Ministry of Primary Industry**, as input to several of their Primary Industries Earthquake Recovery Funded projects. **Ministry for the Environment**, for post-earthquake erosion accounting, as part of New Zealand's commitment to the Kyoto Protocol.
Landslide dam database	Digital geospatial outlines (polygons) of landslide dam locations and their dimensions, which were assumed to have been triggered by the Kaikoura Earthquake, and mapped as part of this research. Including periodic surveys following their failure (breaching) to capture the breach geometry and failure mechanisms, as well as mapping of the downstream impacts from the resultant debris floods. The data is in GIS format.	**ECAN and MDC**, as part of their ongoing hazard management of the potential impacts from dam failure. University of Auckland have used this data, and their students have generated new data to help understand the mechanisms of dam failure.
Landslide debris runout	Landslide debris runout data collated from the Kaikoura Earthquake generated landslides and those generated post-earthquake during significant rain events. Runout is the distance debris travels down slope from its source.	**GNS Science**, as input for the NCTIR alliance – Pilot study for assessing landslide hazards along the road and rail corridors.

Table 3.2 Summary of reports, papers, theses that have used/relied on either funding, or collected information funded by, the emergency post Kaikoura Earthquake, NHRP funded project: Landslide inventory and landslide dam assessments.

Type/date	Organisation/Client/Journal	Affiliation of lead author	Full reference
Paper. In Press.	New Zealand Coastal Society. Special edition	Environment Canterbury	Schoenfeld, M., Massey, C., Dellow, S., Cox, S., McCracken, S., Griffiths, N. 2018. Civil Defence Response to the Kaikoura-Hurunui Earthquake and Tsunami. New Zealand Coastal Society. Special edition. In Press.
Conference paper. June 2018	Eleventh U.S. National Conference on Earthquake Engineering Integrating Science, Engineering & Policy. June 25-29, 2018 Los Angeles, California.	University of Michigan, USA.	Zekkos, D., Clark, M. , Willis, M. , Athanasopoulos-Zekkos, A. , Manousakis, J. , Knoper, L. , Stahl, T. , Massey, C. , Archibald, G. , Greenwood, W. , and Medwedeff, W. 2018. 3D models of the Leader Valley using satellite & UAV imagery following the 2016 Kaikoura Earthquake. Eleventh U.S. National Conference on Earthquake Engineering Integrating Science, Engineering & Policy June 25-29, 2018 Los Angeles, California.
Conference paper. June 2018	Eleventh U.S. National Conference on Earthquake Engineering Integrating Science, Engineering & Policy. June 25-29, 2018 Los Angeles, California.	University of Michigan, USA.	Zekkos, D. , Manousakis, J., Athanasopoulos-Zekkos, A. , Clark, M. , Knoper, L. , Massey, C. , Archibald, G. , Greenwood, W. , Hemphill-Haley, M. , Rathje, E. , Litchfield, N. , Medwedeff, W. , Van Dissen, R.J., Ries, W., Villamor, P., Langridge, R. M., and Kearse. 2018. Structure-from-Motion based 3D mapping of landslides & fault rupture sites during 2016 Kaikoura Earthquake reconnaissance. Eleventh U.S. National Conference on Earthquake Engineering Integrating Science, Engineering & Policy June 25-29, 2018 Los Angeles, California.
M.Sc. Thesis. March 2018	University of Auckland	University of Auckland	Baucke, D. 2018. An accuracy assessment of structure from motion within a complex terrain: Hapuku landslide dam. M.Sc., project. The University of Auckland.
M.Sc. Thesis and data-set. March 2018	University of Auckland	University of Auckland	Merkle, J. 2018. Modelling natural dam seepage with SfM/LiDAR surveying and particle size analysis methods – Hapuku dam, Kaikoura. M.Sc., project. The University of Auckland.
Journal paper. January 2018	Bulletin of the Seismological Society of America	GNS Science	Massey, C.I.; Townsend, D.B.; Rathje, E.; Allstadt, K.E.; Lukovic, B.; Kaneko, Y.; Bradley, B.; Wartman, J.; Jibson, R.W.; Petley, D.M.; Horspool, N.A.; Hamling, I.J.; Carey, J.M.; Cox, S.C.; Davidson, J.; Dellow, G.D.; Godt, G.W.; Holden, C.; Jones, K.E.; Kaiser, A.E.; Little, M.; Lyndsell, B.M.; McColl, S.; Morgenstern, R.M.; Rengers, F.K.; Rhoades, D.A.; Rosser, B.J.; Strong, D.T.; Singeisen, C.; Villeneuve, M. 2018 Landslides Triggered by the 14 November 2016 Mw 7.8 Kaikoura Earthquake, New Zealand. Bulletin of the Seismological Society of America, Online first: doi: 10.1785/0120170305

Type/date	Organisation/Client/Journal	Affiliation of lead author	Full reference
Journal paper. January 2018	Bulletin of the Seismological Society of America	USGS	Allstadt, K.E.; Jibson, R.W.; Thompson, E.M.; Massey, C.I.; Wald, D.J.; Godt, J.W.; Rengers, F.K. 2018 Improving near-real-time coseismic landslide models: lessons learned from the 2016 Kaikoura, New Zealand, earthquake. Bulletin of the Seismological Society of America, Online first: doi: https://doi.org/10.1785/0120170297
Conference paper. November 2017	20th Symposium of the New Zealand Geotechnical Society, Napier 2017	GNS Science	Dellow, G.D.; Massey, C.I.; Cox, S.C. 2017 Response and initial risk management of landslide dams caused by the 14 November 2016 Kaikoura earthquake, South Island, New Zealand. 8 p. IN: Alexander, G.J.; Chin, C.Y. (eds) 20th Symposium of the New Zealand Geotechnical Society, Napier 2017. Wellington, N.Z.: Institute of Professional Engineers New Zealand.
Journal paper January 2018	Bulletin of the Seismological Society of America	University of Durham, UK	Tom R. Robinson, Nick J. Rosser, Tim R.H. Davies, Thomas M. Wilson, Caroline Orchiston; Near-Real-Time Modeling of Landslide Impacts to Inform Rapid Response: An Example from the 2016 Kaikōura, New Zealand, Earthquake. Bulletin of the Seismological Society of America doi: https://doi.org/10.1785/0120170234
Conference paper. November 2017	20th Symposium of the New Zealand Geotechnical Society, Napier 2017	GNS Science	Dellow, G.D.; Massey, C.I.; McColl, S.T.; Townsend, D.B.; Villeneuve, M. 2017 Landslides caused by the 14 November 2016 Kaikoura Earthquake, South Island, New Zealand. 8 p. IN: Alexander, G.J.; Chin, C.Y. (eds) 20th Symposium of the New Zealand Geotechnical Society, Napier 2017. Wellington, N.Z.: Institute of Professional Engineers New Zealand.
GNS Science miscellaneous series. November 2017	8th International INQUA Meeting on paleoseismology, Active Tectonics and archeoseismology	GNS Science	Jones, K.E.; Lawson, S.; Asher, C.; Manousakis, J.; Clark, K.J.; Archibald, G.C.; Ries, W.F.; Massey, C.I. 2017 Rapid RS data collection for landslide damage and fault rupture using UAV and structure-from-motion photogrammetry following the 2016 Mw 7.8 Kaikoura Earthquake. p. 176-179 IN: Clark, K.J.; Upton, P.; Langridge, R.M.; Kelly, K.; Hammond, K.A.T. Proceedings of the 8th International INQUA Meeting on Paleoseismology, Active Tectonics and Archeoseismology: handbook and programme. Lower Hutt, N.Z.: GNS Science. GNS Science miscellaneous series 110.
GeoNet News report. November 2017	GeoNet News 23	GNS Science	Payne, B.; Archibald, G.C.; Massey, C.I.; Dellow, G.D. 2017 Using imagery to map landscape changes. p. 8-9 IN: Page, S. (ed.) M7.8 Kaikoura Earthquake: one year on. Lower Hutt, N.Z.: GNS Science. GeoNet News 23
GNS Science Consultancy Report. October 2017	North Canterbury Transport Infrastructure Recovery (NCTIR)	GNS Science	Massey, C.I., Lukovic, B., Taig, T., Rosser, B, Ries, W. 2017. The North Canterbury Infrastructure Recovery Alliance: Pilot study for assessing landslide hazards along the road and rail corridors. Lower Hutt (NZ): GNS Science. 69 p. (GNS Science consultancy report; 2017/185).

Type/date	Organisation/Client/Journal	Affiliation of lead author	Full reference
Journal paper. June 2017	Bulletin of the New Zealand Society for Earthquake Engineering	GNS Science	Dellow, G.D.; Massey, C.I.; Cox, S.C.; Archibald, G.C.; Begg, J.G.; Bruce, Z.R.; Carey, J.M.; Davidson, J.; Della-Pasqua, F.N.; Glassey, P.J.; Hill, M.P.; Jones, K.E.; Lyndsell, B.M.; Lukovic, B.; McColl, S.; Rattenbury, M.S.; Read, S.A.L.; Rosser, B.J.; Singeisen, C.; Townsend, D.B.; Villamor, P.; Villeneuve, M.; Godt, J.; Jibson, R.; Allstadt, K.; Rengers, F.; Wartman, J.; Rathje, E.; Sitar, N.; Adda, A.-Z.; Manousakis, J.; Little, M. 2017 Landslides caused by the M_w7.8 Kaikoura Earthquake and the immediate response. Bulletin of the New Zealand Society for Earthquake Engineering, 50(2): 106-116
Report. June 2017.	USGS Science Investigation report	USGS	Jibson, R. W., K. E. Allstadt, F. K. Rengers, and J. W. Godt (2017). Overview of the geologic effects of the November 14, 2016 Mw 7.8 Kaikoura, New Zealand, earthquake, U.S. Geol. Surv. Sci. Investig. Rept. 2017-5146.

3.2 Future work

Following completion of this short-term project, mapping of the inventory has continued using reallocated GNS Science Strategic Science Investment funding and later funding from the MBIE Endeavour programme: Earthquake Induced Landscape Dynamics (EILD) programme (see below). Mapping is now near complete and Version 2.0 of the landslide inventory will be made available once the mapping has been checked for consistency. Currently there are more than 20,000 landslide source areas in the inventory (Figure 2.1). These landslides are inferred to have been triggered by the Kaikoura Earthquake and associated aftershocks as no major rain events occurred in the period between the earthquake and the first low-level aerial photograph survey after the earthquake, dated December 2016, used to map the distribution.

This programme is funding five PhD's, one postdoc and four MSc's. It includes team members from Canterbury University, University of Auckland, Victoria University and OPUS engineering consultants, as well as researchers from Simon Fraser University, Vancouver, Canada, the University Durham, Durham, UK, and the Disaster Prevention Research Institute, Kyoto University, Kyoto, Japan.

The landslide inventory has also been used to develop a prototype earthquake-induced landslide forecast tool for New Zealand (Massey and Lukovic, 2018), under the Enhanced Geohazards Monitoring project.

The landslide inventory has been requested and sent to researchers in four international institutions, who are using it for their research in earthquake-induced landslides. Version 1.0 of the landslide inventory (Massey et al., 2018) can be downloaded from the GNS Science landslide database https://data.gns.cri.nz/landslides/ or the https://www.designsafe-ci.org/ website. Version 2.0 of the landslide distribution, will be uploaded later in 2018, once checking of the inventory has been completed.

4.0 ACKNOWLEDGMENTS

This work was funded by the New Zealand Natural Hazards Research Platform. Additional funding was provided by GeoNet and by GNS Science's Strategic Science Investment fund.

The authors would like to thank Nicola Litchfield and Garth Archibald for reviewing earlier drafts of this report.

5.0 REFERENCES

Davies AJ, Sadashiva VK, Aghababaei M, Barnhill D, Costello SB, Fanslow B, Headifen D, Hughes M, Kotze R, Mackie J, et al. 2017. Transport infrastructures performance and management in the South Island of New Zealand during the first 100 days following the 2016 MW 7.8 Kaikōura earthquake. *Bulletin of the New Zealand Society for Earthquake Engineering*. 50(2):271-299.

Dellow GD, Massey CI, McColl ST, Townsend DB, Villeneuve M. 2017a. Landslides caused by the 14 November 2016 Kaikoura earthquake, South Island, New Zealand. In: Alexander GJ, Chin CY, editors. *20th Symposium of the New Zealand Geotechnical Society*; 2017 Nov 23-26; Napier, New Zealand. Wellington (NZ): Institute of Professional Engineers New Zealand. 8 p.

Dellow GD, Massey CI, Cox SC. 2017b. Response and initial risk management of landslide dams caused by the 14 November 2016 Kaikoura earthquake, South Island, New Zealand. In: Alexander GJ, Chin CY, editors. *20th Symposium of the New Zealand Geotechnical Society*; 2017 Nov 23-26; Napier, New Zealand. Wellington (NZ): Institute of Professional Engineers New Zealand. 8 p.

Hamling IJ, Hreinsdóttir S, Clark KJ, Elliott J, Liang C, Fielding E, Litchfield NJ, Villamor P, Wallace LM, Wright TJ, et al. 2017. Complex multifault rupture during the 2016 M_W 7.8 Kaikoura earthquake, New Zealand. *Science*. 356(6334):eeam7194. doi:10.1126/science.aam7194.

Hancox GT, Ries WF, Lukovic B, Parker RN. 2014. Landslides and ground damage caused by the MW 7.1 Inangahua earthquake of 24 May 1968 in northwest South Island, New Zealand. Lower Hutt (NZ): GNS Science report. 89 p + 1 folded map. (GNS Science report; 2014/06).

Hancox GT, Ries WF, Parker RN, Rosser BJ. 2016. Landslides caused by the MW 7.8 Murchison earthquake of 17 June 1929 in northwest South Island, New Zealand. Lower Hutt (NZ): GNS Science. 131 p. + 4 maps. (GNS Science report; 2015/42).

Heron, D.W. (custodian) 2014 Geological map of New Zealand 1:250,000. Lower Hutt, NZ: GNS Science. GNS Science geological map 1. 1 CD.

Keefer DK. 2013. Landslides generated by earthquakes: immediate and long-term effects. In: Owen LA, editor. *Treatise on geomorphology. Volume 5: Tectonic geomorphology.* p. 250-266. doi:10.1016/B978-0-12-374739-6.00091-9250.

Korup O. 2004. Geomorphometric characteristics of New Zealand landslide dams. *Engineering Geology*. 73(1-2):13-35.

Langridge RM, Rowland J, Villamor P, Mountjoy J, Townsend DB, Nissen E, Madugo C, Ries WF, Gasston Canva AJ, et al. 2018. Coseismic rupture and preliminary slip estimates for the Papatea fault and its role in the 2016 M_W Kaikōura, New Zealand, earthquake. *Bulletin of the Seismological Society of America.* doi:10.1785/0120170336.

Litchfield NJ, Villamor P, Van Dissen RJ, Nicol A, Barnes PM, Barrell DJA, Pettinga JR, Langridge RM, Little TA, Mountjoy JJ, et al. 2018. Surface rupture of multiple crustal faults in the 2016 M_W 7.8 Kaikoura, New Zealand, earthquake. *Bulletin of the Seismological Society of America*. doi:10.1785/0120170300.

Massey CI, McSaveney MJ, Taig T, Richards L, Litchfield NJ, Rhoades DA, McVerry GH, Lukovic B, Heron DW, Ries W, et al. 2014 Determining rockfall risk in Christchurch using rockfalls triggered by the 2010-2011 Canterbury earthquake sequence, New Zealand. *Earthquake Spectra*. 30(1):155-181. doi:10.1193/021413EQS026M.

Massey CI, Townsend DB, Rathje E, Allstadt KE, Lukovic B, Kaneko Y, Bradley B, Wartman J, Jibson RW, Petley DM, et al. 2018. Landslides triggered by the 14 November 2016 M_W 7.8 Kaikoura earthquake, New Zealand. *Bulletin of the Seismological Society of America*. doi:10.1785/0120170305.

Massey CI, Lukovic B. 2018. A prototype earthquake-induced landslide forecast tool for New Zealand. In: *The abstract book of MEGE 2018: the 5th International Symposium on Mega Earthquakes Induced Geo-disasters and Long Term Effects.* Chengdu: State Key Laboratory of Geohazard Prevention and Geoenvironment Protection. p. 109-111.

Nicol A, Khajavi N, Pettinga J, Fenton C, Stahl T, Bannister S, Pedley K, Hyland-Brook N, Bushell T, Hamling IJ, et al. 2018. Preliminary geometry, displacement, and kinematics of fault ruptures in the epicentral region of the 2016 M_w 7.8 Kaikoura, New Zealand, earthquake. *Bulletin of the Seismological Society of America*. doi:10.1785/0120170329.

Perrin ND, Hancox GT. 1991. Landslide-dammed lakes in New Zealand – preliminary studies on their distribution, causes and effects. In: Bell DH, editor. *Landslides: proceedings of the sixth International Symposium*; 1992 Feb 10-14; Christchurch, New Zealand. Rotterdam (NL): A.A. Balkema. p. 1457 – 1466.

Rathje E, Little M, Wartman J, Athanasopoulos-Zekkos A, Massey CI, Sitar N. 2017. Preliminary landslide inventory for the 2016 Kaikōura, New Zealand earthquake derived from satellite imagery and aerial/field reconnaissance, version 1, 4 January 2017, Quick Report 1, ver. 1 of the Forthcoming NZ–US Geotechnical Extreme Events Reconnaissance (GEER) Association Report on the Geotechnical Effects of the 2016 Mw 7.8 Kaikōura Earthquake.

Tacconi Stefanelli C, Segoni S, Casagli N, Catani F. 2016. Geomorphological analysis for landslide dams. In Aversa S, Cascini L, Picarelli L, Scavia C, editors. *Landslides and engineered slopes: experience, theory and practice: Proceedings of the 12th International Symposium on Landslides;* 2016 Jun 12-19; Napoli, Italy. Boca Raton (FL): CRC Press. p. 1883 – 1887.

APPENDICES

A1.0 APPENDIX 1 – AIRBORNE LIDAR DATA

Emergency funding was provided by the Ministry of Business Innovation and Employment (MBIE) via the Natural Hazards Research Platform (NHRP) for airborne lidar acquisition after the 14 November 2016 Kaikoura Earthquake. The lidar data was collected between December 2016 and December 2017 by AAM Ltd.

The main uses of the lidar data by the Kaikoura Earthquake landslide team, have been:

During the response:

1. Topographic input for landslide dam breach modelling. One-meter resolution surface models generated from the lidar data are much higher resolution than the original 8 m resolution LINZ model. This meant that we could more accurately forecast the likely areas of debris flood inundation in the event of a catastrophic dam breach. This provided crucial information to the emergency managers, thus reducing the numbers of people potentially affected (e.g., Ote Makura Stream/Goose Bay).
2. Pre- and post-event lidar differencing to calculate landslide volumes along SH 1 – A thin strip of lidar along SH 1 existed before the Kaikoura Earthquake. This pre-earthquake lidar was differenced from the post-earthquake airborne lidar (subtracted one from the other and the tectonic displacement removed) to estimate the volumes of landslides along the road corridor. This data was used by NCTIR in their resilience study to establish future options for SH 1.

During the recovery:

1. Post-dam breach volume calculations and modelling – most of the landslide dams failed following storms in March and April 2017 and April 2018. We have used the repeat airborne lidar surveys after the April 2017 event to quantify the volumes of debris eroded and deposited downstream below the dams after they breached. We have also carried out ground based (terrestrial) lidar surveys, which we have combined with, and compared to, the airborne lidar. This data has allowed us to better calibrate the dam breach models, which can be used to better forecast debris flood inundation in future landslide dam events.
2. Landslide inventory mapping – the lidar has been critical in allowing us to map the extent of the landslide source areas (where the debris originated) and trails (where the debris went), triggered by the earthquake. This is not yet routinely done for landslide inventories from earthquakes elsewhere in the world, and the availability of such datasets greatly enhancing our understanding of the landslide impacts. The Kaikoura Earthquake landslide inventory is now recognised by overseas peers as one of the best earthquake-induced landslide inventories globally.

A2.0 APPENDIX 2 – METHODOLOGY FOR LANDSLIDE INVENTORY MAPPING

A2.1 Landslide inventory mapping team

The main mapping team comprises:

- Chris Massey, Dougal Townsend, Brenda Rosser, Regine Morgenstern, Delia Strong, Corrine Singeisen, Jon Carey and Barbara Lyndsell (GNS Science);
- Marlene Villeneuve and Jonathan Davidson (University of Canterbury);
- Sam McColl (Massey University).

With support from:

- The Geotechnical Extreme Event Response (GEER) team, comprising Joseph Wartman (University of Washington, USA), Ellen Rathje (University of Texas, USA) and Nick Sitar (Berkley University, USA);
- The United States Geological Survey (USGS) landslide team, comprising Jonathan Godt, Randall Jibson, Kate Allstadt and Francis Rengers; and
- The National Science Foundation (USA) funded RAPID collaborative research project being led by The University of Michigan (USA) "Topographic change and cascading hazards following the M_W 7.8 14 November 2016 Kaikoura Earthquake".

A2.2 Objective of the landslide inventory:

To capture the spatial distribution of landslides triggered by the Kaikoura Earthquake, and to provide information for response and recovery activities and to provide a high-quality dataset for future research.

What is the inventory: The inventory captures information on landslide:

3. Type (material and style of movement),
4. Magnitude (areal size, and volume where possible),
5. Runout (distance the debris travels down slope),
6. Connection/interaction with rivers (e.g. occlusions, blockages, buffered),
7. Surface deformation such as evidence of potential/incipient landslides, e.g. areas of cracking or incomplete failures where landslide debris may still be present in the source and has potential to remobilise.

A2.2.1 Value of the dataset

The data will be useful for recognizing immediate hazards (potential for failures/reactivations), outburst floods (dam breaches), short- to longer-term potential for debris flow and valley floor aggradation impacts, sediment budgets for catchments, and assessing landslide causes (i.e. relationships with topography, geology, fault structures, shaking). One of the main uses of this data will be to assess how slopes performed in particular rock and soil (material) types during the earthquake. These data will be especially useful for those similar-sized slopes in Wellington, where much of the city is formed in similar materials (greywacke sandstones and argillites) to those forming the slopes, albeit in the more mountainous Kaikoura region. Such

data will allow us to better constrain the response of the slopes in Wellington to strong shaking e.g. a Wellington Fault earthquake.

A2.3 Data capture and availability

Capturing the landslide data is an ongoing process as new information becomes available (e.g. satellite and aerial images, lidar survey data). It therefore takes time to collate such high-quality landslide datasets. However, we recognize that there is a need to deliver data to stakeholders and other affected parties in a timely manner. To facilitate the transfer of this data, we were originally (in the first few months after the earthquake), sending out near-weekly updates of the inventory to those parties who wanted it. Our intention is to make the inventory freely available to anyone who would like it. At various stages of completion, the inventory will be uploaded to the NZ landslide database maintained by GNS Science. Version 1.0 of the landslide inventory (Massey et al., 2018) can be downloaded from the GNS Science landslide database https://data.gns.cri.nz/landslides/ or the https://www.designsafe-ci.org/ website. Version 2.0 of the landslide distribution, will be uploaded later in 2018, once checking of the inventory has been completed.

The Version 1.0 inventory was compiled in two stages:

1. Initial compilation – based on post event satellite images and georeferenced aerial oblique photographs, along with pre-event orthorectified aerial photographs. Completion February 2017.
2. Revised compilation – Using the initially compiled data, but updated using the post-earthquake orthorectified aerial photographs and lidar data, along with the surface change models generated from lidar and aerial and satellite photogrammetry data (pre- and post-earthquake). Completion date August 2017.

A2.4 Data sources

A summary of the imagery and topographic data used to map the landslide distribution is presented in Appendix 3.

A2.4.1 The initial inventory

The initial compilation was based on the following post-earthquake data:

- WorldView-2 (WV2) 2.4 m resolution (multispectral bands). Imagery date: 22 November 2016;
- WorldView-3 (WV3) is 1.4 m resolution (multispectral bands). Imagery date: 15 November 2016;
- GeoEye (GE) 2 m resolution. Imagery date: 15 November 2016.

The WV2 and WV3 images (provided by Digital Globe) were processed by GNS Science. These have good positional quality (X, Y and Z) but in some mountainous areas the images have been poorly stretched (relief stretch). The same images have been processed by EAGLE Technology. These have better relief stretch but poor positional quality. The images from the different data sources do not cover the entire area affected by landslides, but together they do cover all the main area affected by landslides.

In addition to the satellite imagery, low level aerial oblique photographs were also used to help define the landslides. These (many thousands) of photographs have been captured by the

landslide response team and others post-earthquake, mainly from helicopters. The photographs are georeferenced, and they cover most of the area affected by landslides. They are made available to mapping team via a geodatabase structure in ESRI ArcMap.

The national LINZ 8 m by 8 m digital elevation model (DEM) covers the entire area affected by landslides. This was also used for the mapping. In addition to this, there is also a 1 m by 1 m DEM generated from pre-earthquake lidar. This is confined to a small coastal strip, but it was still useful.

The USGS landslide program team and members of the Landslide GEER team have also contributed their field data collected when they were in New Zealand a few weeks after the earthquake. Some of this information comprises a preliminary landslide inventory based on Landsat imagery (carried out by the University of Texas), which covers some of the main area affected by landslides. These data were also used to generate the initial landslide inventory.

A2.4.2 Revising the initial inventory

The initial compilation was revised once the following data sources were available:

- Post-earthquake orthorectified aerial photographs (captured by Aerial Surveys Limited and commissioned by LINZ), 0.3 m resolution;
- Post-earthquake digital elevation models derived from airborne lidar data;
- Post-earthquake digital surface models derived from stereo satellite imagery (NSF RAPID project);
- Pre- and post-earthquake digital surface models derived from the aerial photographs.

A2.5 Methodology (workflow)

A2.5.1 Landslide inventory geodatabase

To ensure a consistent methodology for capturing landslide information, several feature classes in an ArcGIS geodatabase were set up, with fields containing drop down (restricted) lists for capturing the key landslide information (discussed below).

The wider affected area was roughly divided into broad catchments, with some catchments sub-divided. Each landslide mapper was assigned one or more catchment areas to work in. Landslide mappers were from GNS Science, Massey University and the University of Canterbury, with people from GEER and USGS helping to selectively field truth some of the mapping.

Each mapper worked with a separate copy of the landslide inventory, identified by a unique file name suffix. This was done so that within the geodatabase, for any data added (i.e. feature classes being populated) the work of an individual mappers could be identified by the name or initials in the ‘originator’ field.

After mapping the respective areas (and any weekly/monthly updates generated during mapping), the data was collated into one geodatabase and sent to the various parties who wanted it. For checking, a sample of each area was checked by another mapper. Following this checking, further samples of the mapped data were targeted for field verification, and if needed the landslide feature classes updated.

A2.5.2 Landslide information being collected:

For each landslide, the following information is being collected:

Geodatabase feature classes:

1. Polygons:
    a. Extent of source area (polygon). Note that as best as possible, this should define the whole source area (not just the exposed source area), and may therefore overlap with the landslide debris;
    b. Extent of landslide debris.
2. Points:
    a. Landslide crown: A point at the top of the landslide crown/headscarp (highest point);
    b. Debris Toe: A point at the distal end of debris tail (lowest down slope point).
3. Lines:
    a. Slope deformation: evidence of surficial cracking (scarps), bulging or other deformation indicating mass movement not captured within the landslide polygon areas. These are potential sites of water ingress during later rainstorm events that may destabilize the slope.

Each of these features is linked by a common feature ID, in the 'SourceID' field within each feature class. If there are multiple source areas linked to one debris trail, each Source ID number is added into the 'SourceID' field in the landslide debris attribute table, each entry separated/followed with a comma, but with no space (e.g.: 1002,1003,1004,).

Landslide attributes:

For each landslide source area polygon, as much information as possible is entered into the attribute table. There are drop down lists for landslide type information (material type and movement style/mechanism), which are based on the Hungr et al. (2014)[2] classification. There are other terms that have also been added that are not included in the classification. There are also a few landslide types that are unlikely to occur in the study area (such as peat failures) but they have been included for completeness. Table A2.1 shows the attribute fields for the source area feature class, with an explanation and example of each.

Table A2.1 Landslide source area attributes

Fields	Object ID	Source ID	Primary material	Secondary material
Explanation	Auto	A unique number for each source area.	The main material type that failed. This is not the geology or description of the origin of the material, but rather related to the material properties and their genesis (origin) which influence the failure and runout behaviour.	If there is a second material type involved which appears to have had a significant influence on the failure or runout mechanics, then can include a second material type. If only one major material type, just leave this field as 'Null'
Examples		1000	Rock, clay, mud, coarse clastic (e.g. non-plastic silt, sand, gravel and boulders), peat, ice, undifferentiated	Same options as primary material

[2] Hungr, O., Leroueil, S., Picarelli, L., 2014. The Varnes classification of landslide types, an update. Review article. Landslides. April 2014. Volume 11. Issue 2, pp 167-194.

Table A2.1 Continued

Landslide style	Activity/history	Connectivity	Comment	Method & Confidence
The movement mechanism	Indicate whether landslide appears to be a first-time failure or a reactivation of a previous movement	This describes the relationship of the landslide debris to streams/rivers or major drainage lines.	Additional notes or clarifications	Initial mapping method (i.e. imagery etc) used to digitize the landslide, and confidence in the mapping
Fall, topple, slide (can differentiate into rotational, planar, wedge), flow (can differentiate into avalanche, dry flow, flowslide, earthflow), slope deformation, or creep. Use 'undifferentiated' if you cannot tell which style of movement.		Uncoupled (i.e. sediment has remained on the slope); Coupled (at least some of the sediment has entered a drainage line (including active floodplain, but not including well-vegetated terraces); Blocked (any evidence of blockage even if blockage has since breached)		For each of the methods (Satellite, Orthophoto, Oblique photo, Ground visit, or Multiple [i.e. some combination of these methods]), specify the confidence of the mapping by either 'High' or 'Low'. 'Low' confidence may indicate strong uncertainty in the landslide boundary, uncertainty in the type of landslide mapped, or uncertainty in co-seismic occurrence (in Kaikoura EQ sequence). 'High' confidence can be used if you are confident on the mapping.

Table A2.1 Continued

Shape Area	Length	Geology	Originator
Auto generated	Auto generated	Will auto generate from QMAP data later	Who digitized the landslide
			C. Massey

For the debris trail polygon, and the crown and debris toe point feature classes, only the SourceID is used to link to the landslide source area from where the debris originated.

In addition to discrete landslides, where linear slope deformation features are apparent (i.e. evidence of incipient failures, such as scarps, antiscarps, or cracks that occur outside of the landslide polygons), these have been mapped using the Surface Deformation feature class. In such cases, the only key information added to the attribute table is the type of surface deformation, which is selected from the 'Type' dropdown menu.

Unmapped areas: It is important to know which areas within a designated work area are not able to be mapped, due to e.g., cloud cover or poor-quality imagery. For these areas, a separate polygon shapefile (named 'obscured areas') has been created, which outlines the location of these obscured areas.

A3.0 APPENDIX 3 - SUMMARY OF DATA USED TO COMPILE THE LANDSLIDE INVENTORY

Table A3.1 Summary of data used to compile the landslide inventory.

Item		Data	Type	Date (NZST)	Source	Ground resolution (m)	Notes
Pre-Kaikoura Earthquake data	1	Kaikoura District aerial photographs	Orthorectified mosaics Individual tiled tiffs (provided by Council) converted to one mosaic by GNS Science.	2014-2015	Environment Canterbury (ECAN), (captured by Aerial Surveys)	0.3	
	2	Marlborough District aerial photographs	Orthorectified mosaic Individual tiled tiffs (provided by Council) converted to one mosaic by GNS Science.	2011-2012	Marlborough District Council (MDC), (captured by Aerial Surveys)	0.4	
		Marlborough District aerial photographs	Orthorectified mosaic Individual tiled tiff format files	2015-2016	MDC, captured by AAM Group Ltd.	0.2	
	3	Kaikoura Digital Surface Model (DSM), generated from the photographs taken for 1 and 2.	ESRI Grid file	2014-2015	ECAN, captured by Aerial Surveys Ltd.	1.0	
	4		ESRI Grid file already provided	2014-2015	ECAN, captured by Aerial Surveys Ltd.	10.0	
	5	Airborne lidar	Point clouds converted to Digital Elevation Models (DEMs) and Hillshades by GNS Science	2012	Captured by AAM Group Ltd.	1.0	Only the coastal strip from Ward through to Cheviot
Post-Kaikoura Earthquake data	5	WorldView-2 satellite imagery	Multispectral bands supplied raw. Orthorectified as an Imagine file and converted to mosaics by GNS Science	22 November 2016	Captured by Digital Globe	2.4	EAGLE technology processed the same raw images and provided to all of government.
	6	WorldView-3 satellite imagery		15 November 2016	Captured by Digital Globe	1.4	

Item		Data	Type	Date (NZST)	Source	Ground resolution (m)	Notes
	7	GeoEye satellite imagery		15 November 2016	Captured by Digital Globe	2.0	
	8	Aerial photographs	RGB stereo-tiff files with image coordinates, processed to individual orthorectified images and DSMs by GNS Science. Aerial Surveys to provide complete processed data set	December 2016	Captured by Aerial surveys Ltd. commissioned by LINZ at the request of GNS Science and other New Zealand agencies	0.3	Area covered is the main area affected by landslides and the total area affected by landslides.
	9	Airborne LIDAR	Point clouds converted to DEM and Hillshades by GNS	November to December 2016	Captured by AAM Group Ltd. commissioned by LINZ at the request of GNS Science and other New Zealand agencies	1.0	Only the coastal strip, main faults and Goose Bay provided to date. Additional areas (dam sites) to be provided later.
	10	Terrestrial LIDAR of landslides and landslide dams on the rivers called – Hapuku, Ote Makura, Linton, Conway, Towy, Stanton and Leader	Point clouds, orthorectified images,	November and December 2016 March, April, May and September 2017	Captured by GNS Science	Variable	Multiple surveys of each dam. Several of the dams failed following Cyclone Debbie and Cook, and surveys of these dams were carried out post failure.

A4.0 APPENDIX 4 - LANDSLIDE DAM ASSESSMENT METHODS

A4.1 Regional-scale assessments

Initially all catchments were searched systematically from helicopters and any constrictions located by Geographical Positioning System (GPS), photographed and recorded in a GIS. Expert judgement was initially used to assess the likelihood of dam failure and the potential down-stream consequences, based on past landslide dam performance. These assessments relied on field-estimated parameters such as: 1) dam height; 2) impounded lake area and volume; 3) source material; and 4) upstream catchment area; and 5) the distance a debris flood might travel downstream. These estimates varied considerably from person to person and given that they were estimated remotely from helicopters, the uncertainties on the parameter estimates were large. The reconnaissance also included identifying rivers and streams where multiple dams were present and where the flood could become a cumulative event. From this exercise a list of about thirty of the larger landslide dams was compiled where a breach hazard was assessed as present. This list of dams was then assessed for potential downstream risks, i.e. where people or property were potentially at risk from the rapid failure of the dam and resultant debris flood. This reduced the list to 12 dams (Dellow et al., 2017b).

A process was developed by GNS Science to survey the dams in priority order based on risk, with those dams posing a potential life safety risk being given the highest priority. The life safety issues identified included both occupied buildings (including a campground) and risks to road-users. Seven dams were identified as posing potential life safety risks, and additional data was collected so that rapid or catastrophic failure of the landslide dam could be modelled and the results used to inform those agencies tasked with managing public safety.

To standardise the approach used to assess the likelihood of dam failure, the landslide dams formed by the Kaikoura Earthquake were assessed using the empirically-based dimensionless blockage index (DBI) (e.g. Tacconi et al. 2016, Korup, 2004). The dimensionless blockage index is defined by Equation 1:

$$DBI = \log\left[\frac{A_b \times H_d}{V_d}\right] \quad (1)$$

Where V_d is the volume of the landslide dam, A_b is the area of the upstream catchment and H_d is the height of the dam. Tacconi et al. (2016), suggest three stability domains can be distinguished in a DBI plot: 1) a stability domain with only stable dams; 2) an uncertain stability domain containing stable and unstable dams; and 3) an instability domain. In the dataset presented by Tacconi et al. (2016), dams with DBI ≥3.98 are stable and dams with DBI ≤2.43 are unstable. Korup`s (2004) data show that dams with DBI ≥5 are stable and dams with DBI ≤3 are unstable.

The Tacconi et al. (2016) and Korup (2004) datasets were digitised (Figure A4.1), and the probability of failure (breaching) for dams with different values of DBI calculated (Figure A4.1). The dam volumes, dam heights and upstream catchment areas for the landslide dams triggered by the Kaikoura Earthquake and which posed a potential risk to life were calculated and plotted on Figure A4.1.

Work is currently ongoing under the MBIE Endeavour programme: Earthquake Induced Landscape Dynamics, to calculate the DBI's for all the 196 significant landslide dams, as well as the DBIs for other New Zealand-based landslide dam datasets from e.g., Perrin and Hancox (1991) and unpublished historical landslide dam data held in GNS Science archives.

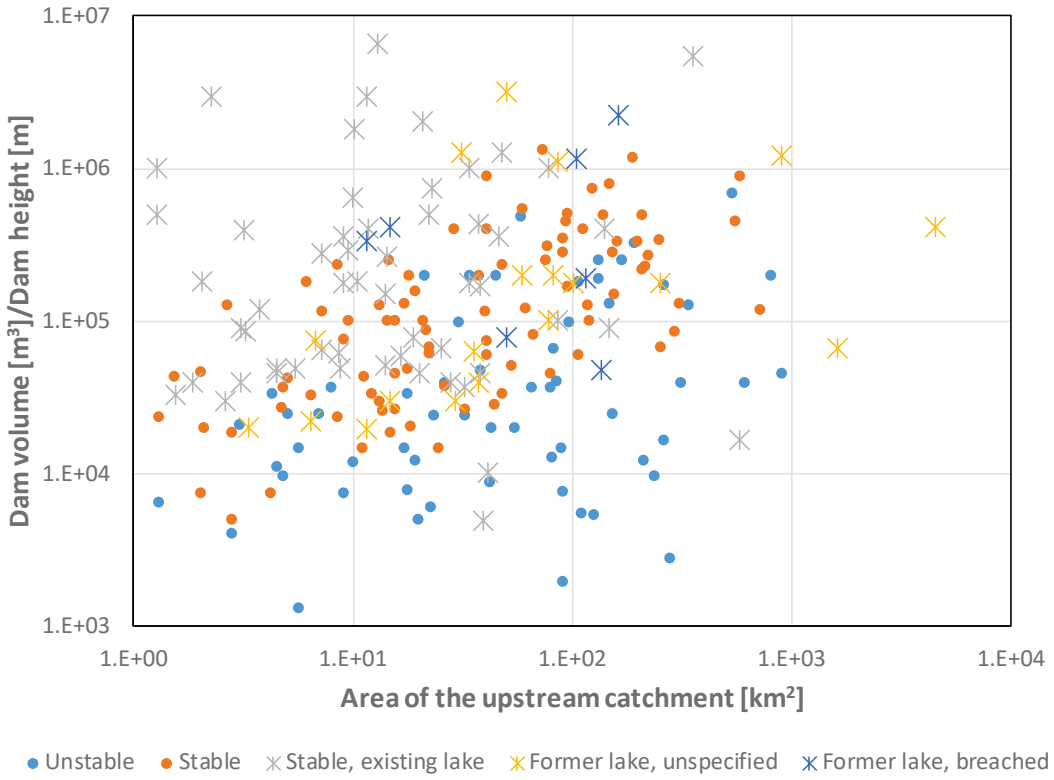

Figure A4.1 Landslide dam volume divided by dam height plotted against the area of the upstream catchment for each landslide dam included in the Korup (2004) and Tacconi et al. (2016) datasets. The red and blue dots represent the Italian dam dataset presented by Tacconi et al. (2016) and crosses represent the New Zealand dataset from Korup (2004). The Italian dataset comprise 152 data points and the New Zealand dataset comprises 85 data points. Total N=238.

A4.2 Site-specific assessments

The assessments comprised:

- Surveys of the dams using airborne and terrestrial lidar at different epochs following major events such as rainstorms and breaching to develop change models between survey epochs (Figure 2.19 to Figure 2.21). Such change modes are used to estimate the volumes of material eroded from the dams and deposited downstream as well as changing dam geometry;
- Field mapping and insitu sampling and testing of the particle size distribution of the debris forming the dams (Figure 2.22), along with mapping of seepage points, seepage flow rates and other pertinent details;
- Field mapping of debris flood heights “trash lines”, downstream of those dams that breached, generating debris flows and floods. This was done to calibrate the landslide dam-breach debris-flood simulations;
- Numerical simulations of dam-breach debris flows and floods. These simulations were calibrated using data collected from the actual dam breach events at the sites (Figure 2.23).
- Monitoring of impounded lake levels, time-lapse photography of the downstream dam faces and downstream river stage levels of several of the dams (on the Hapuku and Linton rivers and the Ote Makura Stream). Although monitoring was originally planned to be carried out via GeoNet, it was in the end carried out by NCTIR and ECAN. This data has captured several of the dam-breach events and resultant downstream flood waves.

www.gns.cri.nz

Principal Location

1 Fairway Drive
Avalon
PO Box 30368
Lower Hutt
New Zealand
T +64-4-570 1444
F +64-4-570 4600

Other Locations

Dunedin Research Centre
764 Cumberland Street
Private Bag 1930
Dunedin
New Zealand
T +64-3-477 4050
F +64-3-477 5232

Wairakei Research Centre
114 Karetoto Road
Wairakei
Private Bag 2000, Taupo
New Zealand
T +64-7-374 8211
F +64-7-374 8199

National Isotope Centre
30 Gracefield Road
PO Box 31312
Lower Hutt
New Zealand
T +64-4-570 1444
F +64-4-570 4657